4
In-Line Product Quality Control of Pharmaceuticals In Freeze-Drying Processes

Antonello A. Barresi and Davide Fissore

4.1
Introduction

Freeze-drying is a process where water (or another solvent) is removed from a frozen product by sublimation. The process consists of three steps: first the product to be dried is frozen; then the pressure is lowered below the triple point to cause ice sublimation (primary drying) while heat is continuously supplied, for example, by conduction through a heated shelf, as the sublimation process is endothermic. Finally, the residual water, strongly bound to the partially dried product, is reduced to a low level by using high vacuum and moderate temperatures (secondary drying), thus ensuring the long term preservation of the product. The low operating temperatures make freeze-drying suitable for highly heat-sensitive products, like pharmaceuticals, that may be damaged by the higher temperature required by traditional drying processes; moreover, freeze-drying warrants a final product that can be easily re-hydrated. Nevertheless, freeze-drying is employed only for valuable goods because of the slow drying rate and the use of vacuum which result in high investment and operating costs (Mellor, 1978; Liapis, 1987; Jennings, 1999; Oetjen and Haseley, 2004; Rey and May, 2004).

Product quality control in a freeze-drying process requires the in-line monitoring of the temperature and of the residual water content of the product. In fact, *product temperature* has to be maintained below a value corresponding to the eutectic point of the system in the case of solutes that crystallize, in order to avoid melting, that is, the formation of a liquid phase, or to the glass transition temperature (T_g') in the case of solutes, such as proteins, that do not crystallize, in order to avoid shrinkage and/or collapse of the cake structure (Franks, 2007). Shrinkage and collapse can be responsible for a higher residual water level in the final product, an extended reconstitution time and the loss of activity of the pharmaceutical ingredient; besides this, a collapsed product is often rejected because of the unattractive physical appearance (Pikal and Shah, 1990; Wang, 2000; Rambhatla *et al.*, 2005). In addition to the temperature, the *residual water content* has to be monitored in order to detect the

Modern Drying Technology Volume 3: Product Quality and Formulation, First Edition.
Edited by Evangelos Tsotsas and Arun S. Mujumdar.

endpoint of the primary drying, so that secondary drying is started only when primary drying is complete: in fact, if secondary drying is started before the sublimation endpoint, the product temperature may exceed T'_g, thus causing collapse in some vials, while if secondary drying is delayed after the sublimation endpoint, the cycle is not optimized and the cost of the operation increases. Finally, the residual water content at the end of secondary drying has to be monitored: for most products the target level of residual water is very low, usually less than 1.0–3.0%, so that the viability, immunologic potency and the stability of the product is not compromised over time. However, for certain products it has been demonstrated that a too low level of residual water should be avoided, as viability, or other characteristics, are compromised by over-drying (Hsu *et al.*, 1992): living cells can lose viability, the tertiary structure of complex proteins can be impaired, with subsequent loss of activity, or, finally, monolayers of water can be removed from active sites on molecules which can then react with traces of oxygen and degrade.

Currently, even the most advanced industrial freeze-dryers have control systems that are no more than data acquisition tools for certain key variables (Liapis *et al.*, 1996). Monitored data and information obtained in previous runs carried out with the same formulation are used to manage the process, assuming that if the operating conditions are the same as used in the validation batches, the same results will be obtained. This statement is false, because neither ingredients nor processing conditions can remain exactly the same, for example, there can be changes from batch-to-batch due to stochastic subcooling, leading to different nucleation temperatures; in some cases the working temperature, as well as the temperature ramp required to reach this temperature, is selected by the operator: this, however, may not guarantee repeatable conditions for the freezing and sublimation steps. In some other cases the operating conditions (temperature of the shelf and pressure in the drying chamber) are selected by means of the mathematical simulation of the drying phase, with the goal to optimize the process (Rene *et al.*, 1993; Lombraña *et al.*, 1993a, b; Boss *et al.*, 2004; Velardi and Barresi, 2008a).

Poor process control is a consequence of the impossibility of measuring in-line the parameters of interest, namely the product temperature and the residual water content. Moreover, regulatory guidance, up to now, has imposed operation of the manufacturing process in an open loop, so that only monitoring was allowed during production. Nevertheless, at least during the phase of process development carried out at laboratory or pilot scale, it would be very useful to have an in-line control system to minimize the drying time: process development can be expensive and time consuming but no regulatory restrictions apply during this phase and, thus, the use of an efficient control system can give significant advantages. Recently, the research in this field has been strongly encouraged by the issue of the Guidance for Industry PAT (Process Analytical Technology) by the US Food and Drug Administration in September 2004. This guidance describes a regulatory framework encouraging the design and implementation of innovative pharmaceutical development, manufacturing and quality assurance to support innovation and efficiency to have safe, effective and affordable medicines. PAT is considered to be a system for designing, analyzing and controlling manufacturing through timely measurements

of critical quality and performance attributes of raw and in-process materials and processes, with the goal of ensuring final product quality: quality cannot be tested into products, but it should be built-in or should be by design. The benefits that can be achieved by an optimal control and monitoring policy have been recently discussed by Sadikoglu *et al.* (2006).

The pressure in the drying chamber and the temperature of the shelf are the two variables that can be used for control purposes, as they affect mass and heat transfer. The pressure can have an opposite effect on the two phenomena: Sandall and Wilke (1967) found experimentally and theoretically that there is an optimal pressure that maximizes the drying rate, while Nail (1980) and Pikal *et al.* (1984) showed that, even if sometimes mass transfer can be the rate-limiting factor, heat transfer from the heat source to the sublimation front is usually the rate-limiting process, as the low pressure reduces the gas thermal conductivity, thus increasing the heat transfer resistance in the air gap between the vials and the shelf (or, if a tray is used, between the vials and the tray and between the tray and the shelf). Nevertheless, the situation seems to be controversial since Jennings (1986), by measuring the sublimation rate of ice, found that decreasing pressure has a positive effect on the sublimation rate. Livesey and Rowe (1987) considered different case studies and pointed out that, even if from a theoretical point of view the sublimation rate is expected to be negatively affected by an increase in the chamber pressure, the enhancement of the heat transfer has a more significant effect. An optimum in the operating conditions can be found as a function of product characteristics: Franks (1998) showed values of the chamber pressure and of the shelf temperature that allow one to maintain the maximum product temperature at a certain level, that can be set equal to the maximum allowable value in order to minimize the drying time. Similar results were given by Oetjen and Haseley (2004) using a simplified model for the main drying, while Trelea *et al.* (2007) used a detailed mathematical model to calculate the value of the shelf temperature that minimizes the drying time, besides maintaining the product temperature below the maximum allowable value; Velardi and Barresi (2008a) included the chamber pressure in the optimization of the process.

During secondary drying the temperature is higher than for primary drying due to the low value of residual water and, thus, the higher glass transition temperature (Franks, 2007). Also, in this case the shelf temperature and the total pressure in the drying chamber can be manipulated in order to minimize the time required to reach the desired amount of residual water in the product, taking into account the constraints on maximum allowable product temperature (Sadikoglu *et al.*, 1998; Sadikoglu, 2005; Pikal *et al.*, 2005; Tang *et al.*, 2005). The variation of the maximum allowed product temperature with the residual water content has been taken into account in the control algorithm proposed by Trelea *et al.* (2007), thus resulting in a further reduction of the drying time.

This chapter aims to discuss various issues concerning the monitoring and control of the three steps of a freeze-drying process of pharmaceuticals in vials, namely freezing, primary and secondary drying. Various devices used to monitor the process, both in pilot-scale and in industrial-scale equipment, as well as the tools proposed to control the process will be described and discussed.

4.2
Control of the Freezing Step

Freezing conditions can strongly influence the primary and secondary drying, as well as the characteristics of the final product, as this step determines the shape and the dimensions of the ice crystals that form the structure of the frozen product (see Chapter 3 for more details). As far as primary drying is concerned, the ice crystals should be large in order to result in a highly porous structure, thus allowing the water vapor to flow from the subliming interface to the drying chamber without a significant resistance; with respect to secondary drying, the ice crystals should be small, so that the specific surface area is high, as this is beneficial with respect to water desorption. The optimal ice crystal size has to be determined with respect to the cost of the whole duration of both primary and secondary drying (Jennings, 1999).

For a given formulation various factors can affect the freezing process, namely the cooling rate, that affects the supercooling degree and the ice nucleation temperature (Searles *et al.*, 2001a), the type of freezing (Patapoff and Overcashier, 2002), and the use of an annealing step (Searles *et al.*, 2001b); Hottot *et al.* (2007) extended the analysis of the parameters that can affect the structure of the ice crystals by investigating the influence of the type of the vial and of the filling height. The differences in the ice morphology are generally related to the nucleation rates and to the nucleation temperatures, that is, to the undercooling and to the thermal gradients inside the solution. It is well known that when the aqueous solution in a vial is cooled below the thermodynamic freezing temperature it remains in a subcooled metastable liquid state until nucleation occurs. The nucleation temperature is distributed around a value below the thermodynamic one, that can depend on the freezing rate, and this causes vial-to-vial variations in the ice crystal structure and, thus, in the drying rate and in the physical properties of the freeze-dried product. This can be one of the most important reasons for batch heterogeneity and can seriously impact monitoring and control of the process.

Control of the nucleation processes is thus a key factor for the optimization of the morphological properties of the freeze-dried matrix. Various techniques have been proposed in the past to control the freezing step, for example, the "ice fog" technique and the use of vibrations. In the "ice fog" technique crystals are introduced in the vials to act as nucleating agents for ice formation in subcooled aqueous solutions. This procedure involves lowering the shelf temperature and cooling the samples to the desired temperature of nucleation; then a flow of nitrogen gas at a controlled high pressure (e.g., 1 bar) is circulated through copper coils immersed in liquid nitrogen and is introduced into the humid drying chamber: ice crystals form and enter the vials due to the increase in pressure, thus causing the nucleation of the solution at the desired temperature (Rowe, 1990; Rambhatla *et al.*, 2004). However, the nucleation event does not occur concurrently or instantaneously within all vials upon introduction of the cold gas into the freeze-dryer, because the ice crystals take some time to enter each of the vials to initiate nucleation, and transport times are likely to be different for vials in different locations within the freeze-dryer. Internal convection

devices may thus be required in an industrial-scale equipment to assist a more uniform distribution of the "ice fog" in the drying chamber.

Vibration has also been used to induce a phase transition in metastable materials. Vibrations sufficient to induce nucleation occur at frequencies above 10 kHz and can be produced using a variety of equipment. Vibrations in this frequency range are often termed "ultrasonic", although frequencies in the range from 10 to 20 kHz are typically within the audible range of humans. Ultrasonic vibration often produces cavitation, that is, the formation of small gas bubbles, in a subcooled solution: in the transient (or inertial) cavitation regime, the gas bubbles rapidly grow and collapse, causing very high localized fluctuations of pressure and temperature, while in the stable (or non-inertial) regime the gas bubbles exhibit stable volume or shape oscillations without collapse. The ability of ultrasonic vibration to induce nucleation in a metastable material is often attributed to the disturbances caused by transient cavitation. Control of the nucleation process can enable the freezing of all unfrozen solutions in a freeze-dryer to occur within a more narrow temperature and time range, thereby yielding a lyophilized product with greater uniformity from vial to vial. The industrial realization of ultrasound nucleation poses some problems: a modified freeze-dryer technology (Telstar, Barcelona) was recently realized (Morris *et al.*, 2004) and demonstrated to improve significantly the whole batch homogenization and to reduce the variations of the sublimation rates, without reducing the protein activity. A nucleation temperature range near the melting point was used, thus confirming that the closer the nucleation temperature is to the melting point, the larger is the size of the ice crystals (Passot *et al.*, 2007). Nakagawa *et al.* (2006) showed that a significant increase in the sublimation rate can be obtained by increasing the nucleation temperature from the average spontaneous nucleation temperature to around $-2\,^{\circ}C$ with ultrasound control. They used an ultrasound transducer that was tightly attached to an aluminum plate placed in thermal contact with the aluminum heat exchanger by clamper fixing and coupled with an ultrasound generator (MW400GSIP, SODEVA, France). The nucleation of the samples was realized by 1 s of ultrasound propagation at a selected temperature during cooling the system at $-1\,K\,min^{-1}$. Work on industrial equipment has shown that this technique has a great potential for application in normal production, evidencing, at the same time, the technical problems that must be solved.

Figure 4.1 shows an example of the results that can be obtained when using ultrasound controlled nucleation in comparison to the case of spontaneous nucleation. The data refer to a freeze-drying cycle of liquid formulations of Human Recombinant Interferon α_{2b}. Freezing was carried out in the "LyoGamma special" industrial prototype by Telstar mentioned above, that was equipped with both standard and forced-nucleation shelves, for comparison. The shelves were initially cooled to $-60\,^{\circ}C$ at approximately $0.3\,K\,min^{-1}$. Samples on the nucleating shelf were forced to nucleate at an average sample temperature of $-4\,^{\circ}C$, while samples on the standard shelf were allowed to nucleate spontaneously. This spontaneous nucleation was observed to occur in the range -8 to $-12\,^{\circ}C$. Primary drying was carried out at $-25\,^{\circ}C$ and 0.1 mbar and secondary drying was carried out at $+25\,^{\circ}C$ for 8 h; the weight of five vials was continuously monitored by means of a balance

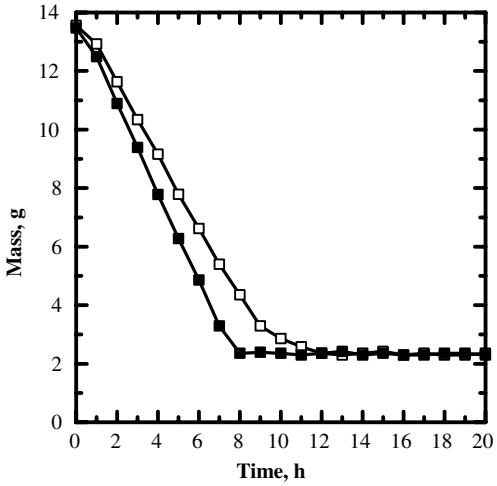

Fig. 4.1 Comparison between the time evolution of the product mass during sublimative drying of a liquid formulation of Human Recombinant Interferon α_{2b} with spontaneous nucleation (□) and with forced nucleation (■).

placed in the drying chamber (see Section 4.3.2). The sharp change in the slope of the curve of the weight of the samples in correspondence to the end of the main drying when forced nucleation is used confirms that the batch is much more homogeneous and the vials terminate the primary drying simultaneously, whereas in the case of spontaneous nucleation some vials end the primary drying before the others, thus resulting in a smooth change of the slope of the curve. The forced nucleation influences not only the duration of the sublimation step, but also the residual moisture at the end of the process: the samples frozen with forced nucleation showed higher residual moisture (0.80% vs. 0.35%) than the samples nucleated spontaneously, while a reduction in the drying time by 43% with respect to the spontaneous nucleation condition was observed. These results are in perfect agreement with the morphology of ice crystals observed for the samples obtained with forced and spontaneous nucleation, respectively. As shown in Fig. 4.2, crystals of larger size are obtained with forced nucleation, so that the mass transfer resistance during the primary drying is lower and the process is faster. During secondary drying a lower active surface is available for the desorption of water and, consequently, a higher residual moisture is obtained than in case of spontaneous nucleation.

4.3
Monitoring of the Primary Drying

After freezing the product, most of the solvent is removed by sublimation during the primary drying. In this stage it is necessary to monitor product temperature and the residual water content in such a manner that the control system can both optimize

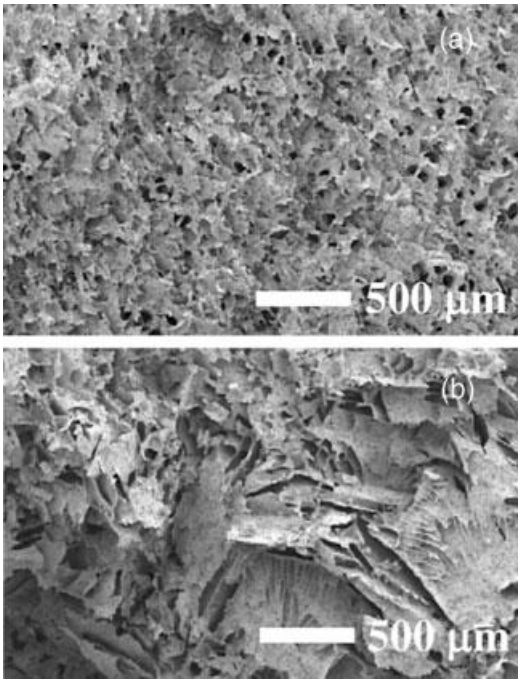

Fig. 4.2 Comparison between the cake structure obtained from a liquid formulation of Human Recombinant Interferon α_{2b} for (a) spontaneous nucleation and (b) forced nucleation; scanning electron microscope, metallized samples.

the process and prevent any damage to the product and any loss of activity in labile materials.

A limitation of the present technology is the impossibility of obtaining in-line measurement of the parameters of interest without interfering with the process dynamics or impairing the sterile conditions usually required when pharmaceuticals are processed. An example of a widespread, but invasive, monitoring device is, in fact, the measurement of the product temperature obtained by inserting a thin thermocouple, or a resistance thermal detector (RTD), inside the vial. While thermocouples are more frequently used in lab-scale equipment, RTDs are preferred in manufacturing due to their mechanical robustness and to the possibility of being sterilized (Willemer, 1991; Oetjen, 1999). Nevertheless, RTDs are usually much larger than thermocouples and the measurement accuracy can be distorted by the sensor geometry (Presser, 2003). The use of thermocouples and RTDs may alter the elementary phenomena of nucleation and ice crystal growth: it is well known that vials where thermocouples or RTDs are placed tend to show a lower degree of supercooling than the surrounding vials and, therefore, form fewer and larger ice crystals which, finally, results in lower product resistance to mass transfer and shorter drying time in comparison to the rest of the batch. While this difference may be inconsequential in the laboratory, the sterile and particle-free environment in

manufacturing leads to substantially higher supercooling of the solution, resulting in larger differences between vials with and without temperature sensors. Moreover, the insertion of even thin thermocouples affects the heat transfer to the product and the probe insertion compromises the sterility of the product and is not compatible with automatic loading/unloading systems used in industrial-scale freeze-dryers (Nail and Johnson, 1991; Schneid and Gieseler, 2008). The development of wireless systems can make the use of the product probes compatible with automatic loading systems, even if all the other concerns remain valid.

Wireless solutions ("active transponders") have been available for about two decades, using the ISM-frequency-bands for short-range data transmission from the sensor-units, and start to be suitable for use in freeze-dryers; however, these active transponders show similar problems to RTDs. Moreover, all of them require batteries for sensor-operation and data-transmission, thus resulting in limited operating time dependent on battery capacity and, finally, unpredictable risks when using batteries in a sterile environment. Recently, a new generation of wireless probes was developed ("passive transponders") which generate the energy required for transmission from an electromagnetic field instead of using batteries (Hammerer, 2007). The temperature remote interrogation system (TEMPRIS) sensors have been recently proposed by Schneid and Gieseler (2008): this system allows real-time temperature measurement at the bottom center of a vial (if placed correctly) and is beneficial for scale-up, as the same sensors can be used in the lab and on a manufacturing scale. The main drawback concerns the placement of the sensor at the bottom center of the vial: this was found to be crucial to obtain reliable temperature profiles and endpoint monitoring, but no "brackets" are available at the moment to assure "bottom center" position. Moreover, the dimension of the sensor is a problem, as well as the fact that the thermocouple is invasive with respect to the product in the vial.

Despite the various drawbacks listed above, thermocouples have been proposed to monitor the primary drying and to detect the endpoint of this stage. When the primary drying ends, an increase in the product temperature is measured at the bottom of the vials due to the loss of thermal contact between the sensor and the ice. Moreover, the product temperature increases as there is no longer an endothermic sublimation process that uses the heat supplied by the heating shelf.

The product temperature can be used to detect the end of primary drying also using a completely different procedure, by regularly and drastically reducing the pressure in the chamber: if no decrease in the product temperature is observed as a consequence of the pressure reduction, that in the presence of residual ice would cause an increase in water flux by endothermic sublimation, then the primary drying can be considered complete (Thompson, 1988).

Finally, by coupling a mathematical model of the process to the measurement of the product temperature in the vial (or of the wall temperature of the vial) it is possible to build a soft-sensor that allows estimation in-line of the whole product temperature profile and the mass/heat transfer coefficients; this has been called the "smart-vial" concept (Barresi *et al.*, 2007, 2009a, b, c)

Non-invasive monitoring techniques have been proposed as valuable alternatives to the use of thermocouples. Most of them are based on the results obtained from the

pressure rise test (PRT): they use the in-line measure of the pressure rise occurring when the valve placed between the drying chamber and the condenser is closed for a short time interval (typically from 5 to 30 s) and estimate the temperature of the sublimating interface and, generally, also other parameters, using a mathematical model of the process. This technique was well known already in the early 1960s (see, for example, Rieutord, 1965), but has only recently been refined to obtain more accurate and reliable results. Several algorithms have been proposed in the literature to interpret the PRT, namely the barometric temperature measurement (Willemer, 1991; Oetjen, 1999; Oetjen *et al.*, 2000; Oetjen and Haseley, 2004), the manometric temperature measurement (Milton *et al.*, 1997; Tang *et al.*, 2006a, b, c), the dynamic pressure rise (Liapis and Sadikoglu, 1998), the pressure rise analysis (Chouvenc *et al.*, 2004, 2005; Hottot *et al.*, 2005) and the dynamic parameters estimation (Velardi *et al.*, 2008). The sublimation flux of the solvent can be calculated from the mathematical model used to fit the curve of the pressure rise or from the slope of the curve of the pressure rise at the beginning of the test (Fissore *et al.*, 2011a) the two procedures should of course give similar results and this can be used as a consistency check (Pisano, 2009; Pisano *et al.*, 2009). By integration of the solvent flux it is possible to calculate the residual ice content of the solid, thus detecting the endpoint of primary drying.

Moisture sensors, mass spectrometer, windmill sensor, pressure gauges and other devices have been proposed in the past to monitor the primary drying and to detect the end of this stage: a technical comparison of these and other recently proposed devices is given in Mayeresse *et al.* (2007), Wiggenhorn *et al.* (2008) and Barresi *et al.* (2009a). All these sensors do not provide any information about the status of the product during the operation and, thus, they cannot be used in a control loop, but they may be very useful to establish when primary drying is completed and secondary drying can be started without causing quality loss.

The various techniques available to monitor the primary drying can be roughly divided into three groups as they can be used to monitor single vials, a group of vials or the whole batch (Barresi *et al.*, 2009a): these techniques will be discussed and compared in the following sections.

4.3.1
Monitoring of Single Vials

Besides the use of thermocouples and RTDs, various other techniques have been proposed to monitor freeze-drying in a vial. A quick mention can be made of the various analytical techniques, such as low-temperature X-ray powder diffractometry (Cavatur and Suryanarayanan, 1998), low-resolution pulse nuclear magnetic resonance (Monteiro Marques *et al.*, 1991), FTIR spectroscopy (Remmele *et al.*, 1997), and visual microscopic observation (Mackenzie, 1964), that have been used for *in situ* characterization of samples being lyophilized in special lyophilization equipment, connected to the analytical instrument. These techniques are very useful for process understanding and process design, but at the moment it seems very difficult to use them in a conventional freeze-dryer.

Removal of samples during the process using a manipulator is a technique, proposed and recommended as an independent control procedure, to follow the sublimation of water (and also the desorption of bound water in secondary drying) especially in the case of very expensive products, such as those produced by genetic engineering and biotechnology; but it is generally employable only in scouting tests, where, on the other hand, it can also allow a step-by-step optimization of the entire process (Willemer, 1987). Of course, sampling can be coupled with any analytical technique available at-line to measure the residual ice or residual moisture, such as gravimetry, titration, spectroscopic methods (Skibsted, 2006) and even X-Ray photography (Schelenz *et al.*, 1994).

The use of sensors based on spectroscopy methods has been investigated for in-line monitoring. Near-infrared (NIR) spectroscopy has been proposed for monitoring the process because the physical changes occurring, that is, freezing, sublimation and desorption, generate significant spectral changes (Presser *et al.*, 2002a; Brülls *et al.*, 2003; Presser, 2003). NIR allows a non-invasive, non-destructive and rapid moisture determination and offers a wide range of capabilities in the process analytical technology of freeze drying pharmaceuticals (Ciruczak, 2002). The end of the primary and secondary drying process can be determined precisely. Moreover, the freezing point, the ice formation process and the transition from frozen solution to dried material can be observed. Good agreement between NIR spectroscopy and product temperature monitoring of the freezing process and of the transition from the frozen product to the ice-free material has been reported (Brülls *et al.*, 2003). The major advantage of this method is the simultaneous and rapid *in situ* process monitoring for process and product conditions resulting in the direct determination of the moisture during different drying stages (Presser *et al.*, 2002a). Wiggenhorn *et al.* (2005a, b, 2008) showed results obtained by locating the NIR sensor on the shelf inside the drying chamber and directly fitted with the probe tube to the outer wall of the vial: this arrangement offered the advantage of sterility compared to other set-ups, where the single fiber reflectance probe of the FT-NIR probe is located inside the vial in combination with a thermocouple (Brülls *et al.*, 2003). It is, furthermore, much less disturbing as it does not affect the drying kinetics of the sample vial nor does it restrict the fill volume or the vial type. Recent studies have described a non-invasive, in-line and real-time analysis of the lyophilization process by means of Raman spectroscopy: De Beer *et al.* (2007) reported some results on the in-line characterization of physical phenomena (i.e., mannitol crystallization) in a lab-scale apparatus, using a fiber-optic non-contact probe placed above the freeze-dried product; they also evidenced the utility of coupling in-line Raman spectroscopy with at-line NIR spectroscopy and X-ray powder diffraction.

Besides spectroscopy methods, other techniques have also been proposed for the in-line monitoring of the water content in single vials: among them, dielectric measurements (Suherman *et al.*, 2002) seem the most promising, at least for detection of the endpoint; the electrodes can be placed outside the vial to reduce interference with the process. Monitoring of electric properties, and in particular of the product resistance (or inductance), has also been proposed. The technique seems suitable especially for substances that show a sharp eutectic melting, as in this case

there is a very large variation in the resistance when the product approaches the limit temperature. The sensitivity of the technique is very high, even if applicable easily only to certain crystalline products, but electrodes must be inserted in the vials: thus, it has been employed mainly for detection of the product critical temperature. Notwithstanding the limitations described, and some reliability problems, resistance monitoring was proposed also for the automatic control of the whole operation, and this will be briefly discussed in a later section (Rey, 1961; De Luca and Lachman, 1965; Jennings, 1999).

Jennings and Duan (1995) developed a different technique to monitor the primary drying, based on the determination of the total energy necessary to carry out the primary drying and on calorimetric measurement to calculate the heat transfer coefficient in the monitored vial, and thus the rate of heat transport. For this purpose a differential method, called drying process monitoring (DPM), is used: two thermocouples are fixed to the bottom of an empty vial and a vial filled with the product, thus allowing calculation of the heat transfer to the filled vial used for the sublimation of ice; a drop in the heat transfer rate can be observed at the end of the main drying (Jennings, 1999). This method requires the introduction of two vials with thermocouple connections in the production batch; thus, even if more sophisticated, and probably more reliable, than the simple measurement given by one thermocouple, the DPM maintains most of the drawbacks of the thermocouples, including the obvious fact that measuring the situation in the two special vials may not represent an average of all the batch vials.

Another device that makes use of the measurement of the temperature of the product (or of the vial) is the soft-sensor (or observer): it provides a real-time estimation of some parameters or state variables, for example, the whole product temperature profile and the mass and heat transfer coefficients, using the temperature measure and a mathematical model of the process. Let us consider a dynamic system defined by the following set of differential equations:

$$\dot{\mathbf{x}} = \mathbf{f}(\mathbf{x}, \mathbf{u}) \tag{4.1}$$

where $\mathbf{x} \in \mathbb{R}^n$ is the state of the system, $\mathbf{u} \in \mathbb{R}^m$ is the vector of the control variables and $\mathbf{f}$ is an application from $\mathbb{R}^n \times \mathbb{R}^m$ to $\mathbb{R}^n$ giving the derivatives of the state as a function of the state itself and of the control law $\mathbf{u}$ applied to the system. In order to build an observer some information concerning the measured variables is required: in this way the equations describing the dynamics of the system become the following:

$$\begin{cases} \dot{\mathbf{x}} = \mathbf{f}(\mathbf{x}, \mathbf{u}) \\ \mathbf{y} = \mathbf{h}(\mathbf{x}, \mathbf{u}) \end{cases} \tag{4.2}$$

where the components of the vector $\mathbf{y} \in \mathbb{R}^q$ are the measured variables and the equation $\mathbf{y} = \mathbf{h}(\mathbf{x}, \mathbf{u})$ involves the description of these quantities in terms of the components of the state vector and of the control law. The observer for the system described by Eq. 4.2 is another system of equations, whose state is denoted by $\hat{\mathbf{x}}$:

$$\begin{cases} \dot{\hat{\mathbf{x}}} = \mathbf{f}(\hat{\mathbf{x}}, \mathbf{u}) + \mathbf{K}(\mathbf{y} - \hat{\mathbf{y}}) \\ \hat{\mathbf{y}} = \mathbf{h}(\hat{\mathbf{x}}, \mathbf{u}) \end{cases} \tag{4.3}$$

where $\hat{\mathbf{y}}$ are the estimations of $\mathbf{y}$ obtained from the observer and $\mathbf{K}$ is the gain of the observer, that is, a non-linear function of the state ($\hat{\mathbf{x}}$) and of the input ($\mathbf{u}$) that ensures asymptotic stability, driving the estimation error $\varepsilon = \mathbf{y} - \hat{\mathbf{y}}$ to zero. The synthesis of an observer, that is, the calculation of the gain $\mathbf{K}$, is a complex task and a lot of algorithms have been proposed in the literature. The Extended Kalman Filter is one of the most common techniques (Becerra *et al.*, 2001) and it has been used to track the freeze-drying process by Barresi *et al.* (2009b) and Velardi *et al.* (2009): they used a simplified pseudo-stationary model and the measurement of the product temperature at the bottom of the vial to estimate the temperature and the position of the moving front as well as the heat and mass transfer coefficients. As an alternative, a High Gain observer has been designed and tested as, in this case, the mathematical formulation is simpler and the computational time required for the estimation is generally lower; moreover, the High Gain observer exhibits less sensitivity towards noisy measurements (Velardi *et al.*, 2010). Both soft-sensors have been validated by numerical simulations using a detailed one-dimensional model as a source of experimental data (Barresi *et al.*, 2009a): the quality of the estimations given by both observers has been verified to be roughly the same, but the computational effort required by the Kalman Filter is higher and its tuning is quite tricky, while the estimations obtained using the High Gain observer are provided faster and the tuning is simpler. Preliminary experimental results confirm that in-line estimations can be very good, as is evidenced in Fig. 4.3, which shows the prediction of the interface temperature and the position of the frozen interface obtained using the Kalman Filter. The main drawback of using an observer to monitor

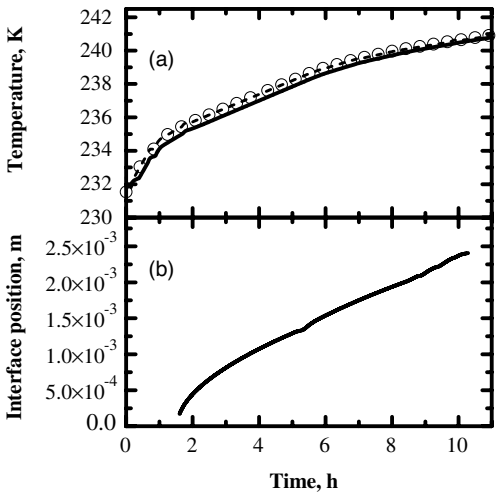

Fig. 4.3 Measurements and estimations of the product temperature and of the moving front position during the FD of 10% w/w sucrose solution ($d_v = 14.2 \times 10^{-3}$ m, $L_p = 7.2 \times 10^{-3}$ m, $P_c = 10$ Pa). (a) Product temperature at the moving front (solid line) and at the bottom (dotted line) estimated using the Kalman filter; (o) temperature at the bottom of the product measured by a thermocouple. (b) Interface position estimated by the Kalman filter (solid line) from the temperature measurement given in the upper graph (Velardi *et al.*, 2009).

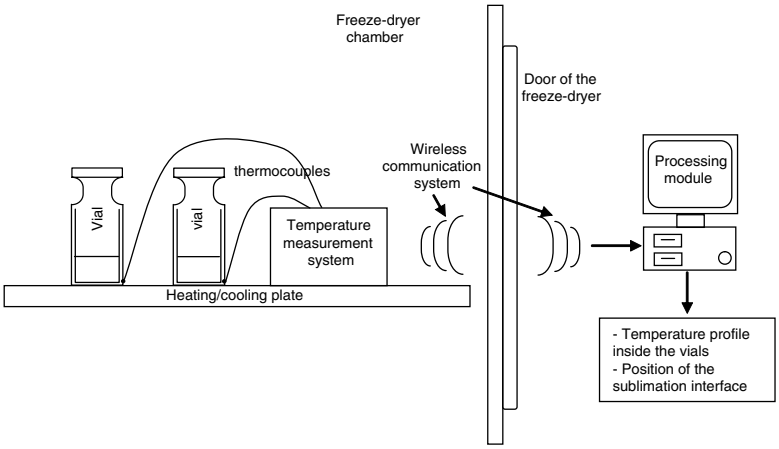

Fig. 4.4 Sketch of the "smart vial" concept, the system using the soft-sensor to monitor the freeze-drying process (Barresi *et al.*, 2007).

the process is that the state estimation is limited to a single vial. On the other hand, the temperature estimation concerns the entire temperature profile of the product in the vial and not only the temperature at a particular point, as is obtained using a thermocouple. Moreover, the results obtained for a particular vial can be compared to those obtained for other vials placed in different positions in the drying chamber, thus allowing evaluation of the heterogeneity of the batch.

Since the insertion of a probe, although extremely tiny, in contact with the product should be avoided because of the various drawbacks previously discussed, a different observer can be designed, using the measurement of the external temperature at the bottom of the vial (Barresi *et al.*, 2007, 2009b, c) and a mathematical model that takes into account also the heat transfer in the glass wall (Velardi *et al.*, 2005; Velardi and Barresi, 2008a). This is the "smart vial" that has been patented recently by Barresi *et al.* (2007). A wireless system, using an active or passive transponder, can be used to transmit measured values to a PC. The passive device (Fig. 4.4) is able to perform temperature measurements in several vials and to communicate the results to an external receiver through a central unit. The low-frequency RF-ID technology is employed in order to avoid the use of batteries (Vallan *et al.*, 2005a). A second kind of device has been recently designed and tested: it makes use of a small battery that can be completely embedded in the vials and is able to transmit the measurements within a range of several meters by means of a 2.4 GHz radio (Barresi *et al.*, 2009b; Fissore *et al.*, 2009c; Corbellini *et al.*, 2010).

4.3.2
Monitoring of a Group of Vials

While the sensors described in the previous paragraph allow monitoring of only single vials, a balance placed directly in the vacuum chamber of the freeze-dryer allows monitoring of a group of vials: the direct weight measurement enables the

tracking of primary drying and detection, with good accuracy, of the endpoint of this stage. Remarkable improvements can be obtained with respect to sample-extractors (Nail and Gatlin, 1993; Tang and Pikal, 2004) as the vacuum conditions are not modified and the weighing procedure is performed in an automatic way. Initially proposed in food freeze-drying processes (Oetjen *et al.*, 1962), were different types of balances to weigh one or more vials in line. Bruttini *et al.* (1986, 1991) proposed a balance which supported the heating plate and the tray: freezing was carried out as a separate step because when it was carried out *in situ*, the vibrations induced by fluid pulsation from the cryostat severely disturbed the measurement. A certain drawback of weighing devices is that the measurement cannot be representative of the process because the weighed vials are exposed to different thermal conditions than the rest of the batch. In the capacitive balance proposed by Rovero *et al.* (2001) the heat transfer to the product is limited by the volumetric gap that acts as an additional resistance when heat is transferred through the shelf by conduction, while it works efficiently in the case of radiative heating. Moreover, some of the balances so far proposed require vials with a specific geometry that does not always correspond to that of the vials of the batch, and the measurement is limited only to that special vial (Christ, 1995; Roth *et al.*, 2001; Gieseler, 2004; Gieseler and Lee, 2008a, b).

Vallan et al. (2005b) proposed and patented a weighing device that works inside the vacuum chamber: it is composed of a motorized balance which is able to rise and weigh several vials (up to 15 small vials in the first prototype, but extensible even to a much larger number and adaptable to different sizes of vials with a proper loading cell), and a miniaturized radio-controlled thermometer, connected to the balance tray, that can measure the temperature of these vials without altering the mass measurement because of the force transmitted by the thermocouple wires, as is sketched in Fig. 4.5 (Vallan, 2007).

Since these vials are almost always in contact with the shelf and lifted just during the measurement, the thermal exchange between the vials and the heating surface is not significantly affected and, therefore, the measurement is representative of the whole batch. The balance is connected to a PC by means of a serial interface; it has a resolution of about 10 mg and a total uncertainty of about 100 mg from -40 to $+40\,^{\circ}$C. A series of tests has shown that the weighing frequency can be chosen in a wide range without affecting the process, but both the monitored vials and the

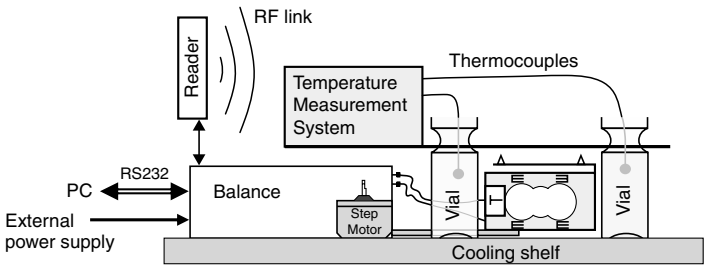

Fig. 4.5 Sketch of the balance for freeze-dryers (Vallan *et al.*, 2005b; Vallan, 2007).

balance case must be properly shielded to avoid systematic errors due to radiation effects from the walls: if this is not done, the vials lifted by the balance are in a condition similar to that of the vials at the sides of the batch, where radiation effects are much more important, and the balance response can be considered representative of this fraction of vials (Pisano *et al.*, 2008). This device has been tested in various freeze-drying cycles performed in different working conditions: a good agreement between the time evolution of the values of mass and temperature has been evidenced during these runs. Figure 4.6 shows an example of the results that can be obtained; the measure of the temperature obtained by means of thermocouples placed at the bottom of some vials is also shown for comparison, as well as the calculated average sublimation rate. When the mass of the vials weighed by the balance becomes very low and almost constant, it means that the endpoint of primary drying has been reached; of course, the calculation of the sublimation rate from the derivative of the mass measurement increases the sensitivity and allows determination of the end of primary drying with good accuracy. The end of the sublimation drying in Fig. 4.6 is confirmed by the strong increase in the product temperature occurring at the same time.

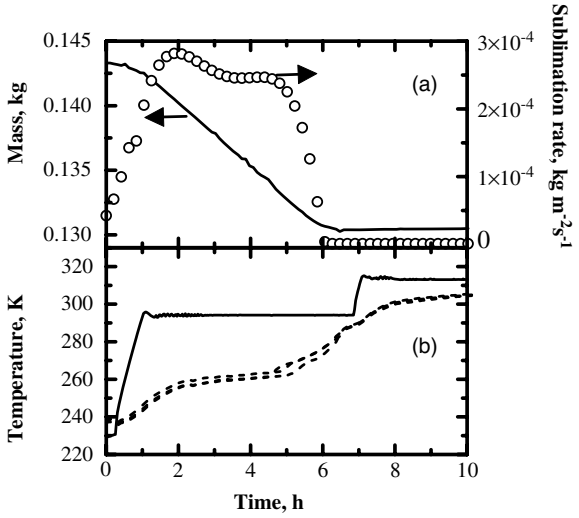

Fig. 4.6 Example of results obtained during a freeze-drying cycle using the special balance with the embedded wireless temperature measurement in order to monitor the primary drying stage of a mannitol-dextran solution (6–14% by weight) in a pilot-scale freeze-dryer. The freezing stage was run at 223 K for about 5 h, while the main drying was carried out setting the fluid temperature at 293 K and the chamber pressure at 10 Pa ($N_v = 98$ on tray, $d_v = 14.2 \times 10^{-3}$ m, $L_p = 7.2 \times 10^{-3}$ m). (a) Time evolution of the product mass (line: the gross mass of 15 vials containing 1 cm^3 of solution each, including glass vials and tray) and average sublimation rate calculated from this measurement (symbols). (b) Time evolution of the heating fluid temperature (solid line) and of the product temperature measured by thermocouples inserted close to the bottom in three of the vials weighed by the balance (dashed lines).

4.3.3
Monitoring of the Whole Batch

As stated in Section 4.1, it is necessary to monitor product temperature in order to avoid collapse (or melting) of the product, and also to detect the end of primary drying, in order to start secondary drying when all the vials have completed their main drying: if secondary drying is delayed the total duration of the cycle, and thus its cost, is increased, while if secondary drying is started before the sublimation endpoint, the product temperature is increased too early and may thus exceed T'_g and cause the product to collapse in some vials. The sensors that can be used to monitor the whole batch can be roughly divided into two groups, those that allow detection only of the endpoint of the primary drying and those that also allow estimation of the product temperature and the residual water content from the results of the pressure rise test (PRT); the latter can be used in a control loop to optimize the primary drying step.

4.3.3.1 Detection of the Endpoint of the Primary Drying

A capacitance manometer or a thermal conductivity gauge, like the Pirani gauge, can be used to measure the pressure in the drying chamber: the latter is cheaper than the capacitance manometer, but the accuracy is generally lower and the signal depends on the gas type and, in the case of mixtures, like water and inert gas, on the composition. Thus, the use of Pirani (and generally of all the thermal conductivity gauges) should be discouraged for monitoring freeze-drying because the chamber gas composition changes continuously during each run and is generally different in different cycles as it depends on set-up, loading and product features (Armstrong, 1980). On the other hand, taking into account the known dependence of the Pirani response on the water vapor fraction, it is possible to evaluate the partial pressure of water in the drying chamber using the signals obtained from the capacitance manometer and from the Pirani sensor. Moreover, as suggested by Nail (Armstrong, 1980; Nail and Johnson, 1991), it is possible to detect the end of the primary drying as the concentration of water into the drying chamber becomes very low at that point and, thus, the pressure measured by the Pirani (that is generally calibrated for air) approaches that measured by the capacitive gauge. The use of the ratio of the pressure signals given by the two gauges, that approaches unity at the end of the primary drying, instead of the simple measure given by the Pirani sensor, is more reliable because it eliminates the possible effect of a variation in the total pressure. It must be taken into account that the method is quite sensitive, and senses the last vials to dry; this is generally desirable, but there is the possibility that some vials in an abnormal configuration, such as vials that fall off the shelf and thus dry much more slowly than regular ones, are responsible for a misleading signal (Nail and Johnson, 1991). One possible limitation to the application of this simple method is the restriction in the use of thermal conductivity gauges in equipment where steam sterilization is required, even if producers claim that new models using different materials for the filament (nickel or platinum rather than the standard tungsten) can cope with sterilization. Recently, new sensors based on the same principle as the Pirani gauge have been proposed: a stainless steel shield is used to

protect against condensation and a pulsed mode of operation allows higher signal resolution, an extended range of measurement and higher long-term stability (Ploechinger and Salzberger, 2006).

An early method used for measuring the partial vapor pressure in the chamber is that of the vapor sampling condensing (or trap method), described in detail by Kan (1962). It is still used, especially in small apparatus for research (Pikal *et al.*, 1984; Roy and Pikal, 1989).

Moisture sensors and mass spectrometers can be used to monitor the time evolution of the water concentration in the chamber. Dew point sensors can detect the gas composition or the relative humidity owing to a change in the dielectric constant of a gold sputtered foil material: they indicate a sharp decrease in the dew point when the water vapor decreases to almost 0% (Bardat *et al.*, 1993) and can have greater sensitivity than a thermal conductivity gauge. Roy and Pikal (1989) used a moisture sensor that exploits the variation of the capacity of a thin film of aluminum oxide due to moisture (Ondyne, by Endress + Hauser HydroGuard 2250, Greenwood, IN): according to the authors, the sensor has the sensitivity to determine the presence of ice in less than 1% of the vials of the batch. This device, first proposed by Bouldoires (1969), was successively used by Genin *et al.* (1996) and by Rambhatla *et al.* (2004) to monitor the process and to detect the sublimation endpoint; Trelea *et al.* (2007), Chouvenc *et al.* (2004) and Barresi *et al.* (2009a) used a similar moisture sensor, developed by Panametrics. Genin *et al.* (1996) also developed a procedure that led to a patented method (Rene *et al.*, 1995) for the estimation of the residual water content in the product at any time during the process.

The use of a radio frequency mass-spectrometer with rapid response (Favitron by E. Leybold's Nachfolger) to detect the end of primary drying (and also of secondary drying) was described by Kan (1962), evidencing that it was able to work even in the absence of inert bleeding. Later, the use of a quadrupole mass spectrometer (QMS) to monitor primary drying was reported by several authors (Jennings, 1980, 1999; Nail and Johnson, 1991; Willemer, 1991; Connelly and Welch, 1993; Presser *et al.*, 2002b; Wiggenhorn *et al.*, 2005a, b). The working principle of a QMS is simple: the gas is sampled to the instrument where the molecules are fragmented, ionized and accelerated by an electric field; the ions are then driven to the detector which gives a signal proportional to the concentration and to the type of the impacting fragment. It is quite difficult to get quantitative measurements as it is not easy to calibrate the instrument for gaseous mixtures with water; moreover, it is necessary to repeat the calibration before each run as the response factor of the instrument can be variable; for this purpose, Jennings (1980) suggested the use of a capacitance manometer to make the calibration. Nevertheless, significant information can be obtained from the QMS even if only the crude signals, given in terms of ionic currents, are investigated: the time evolution of the ionic current corresponding to the fragment of mass 18 (i.e., water), i_{18}, divided by the total pressure reading made by the QMS, was proposed by Jennings (1980) to detect the end of the primary drying: this signal is almost constant during all the primary drying and decreases at the endpoint. With the implementation of an aseptic sterile filter between the drying chamber and the QMS, this device can also be used in commercial scale production set-ups where full aseptic conditions

are mandatory (Wiggenhorn *et al.*, 2005a, b). Despite the high sensitivity and the possibility of also monitoring freeze-drying processes with organic solvents, a QMS is very expensive and, in the common case of just water solvent, it does not provide more "information" than the ratio between the pressure measured by the Pirani gauge and by a capacitance manometer. The QMS may be extremely valuable for quality control, as it can also be used as a diagnostic tool for system leak detection, back-streaming of pump oil, out-gassing of elastomeric components of the freeze-dryer and sublimation of low molecular weight formulation components (Leebron and Jennings, 1981; Nail and Johnson, 1991).

Figure 4.7 shows an example of a freeze-drying cycle where various previously described sensors have been used to monitor the process; in this case a relatively

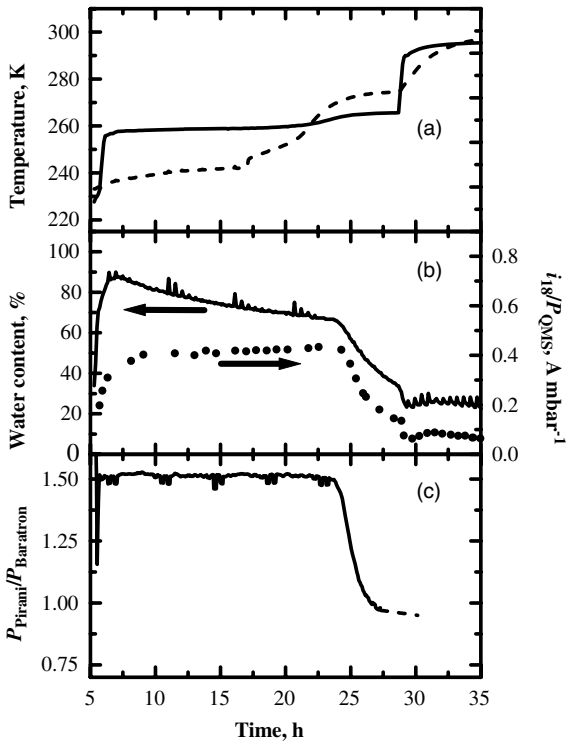

Fig. 4.7 Example of the results obtained during a freeze-drying cycle using various devices to monitor the primary drying stage of 5.5% by weight lactose solution in a pilot-scale freeze-dryer (Barresi *et al.*, 2009a). The freezing stage was run at 223 K for about 5 h, with an initial cooling rate of 1 K min^{-1}, while the primary drying was carried out at 263 K, with $P_c = 10$ Pa ($N_v = 713$ on tray, $L_p = 7.2 \times 10^{-3}$ m, $d_v = 14.2 \times 10^{-3}$ m). (a) Bottom product temperature measured by a thermocouple (dashed line) and heating fluid temperature (solid line). (b) Moisture content in the chamber measured by Panametrics moisture sensor (Panametrics MMS35, solid line) and ratio between the ionic current of mass 18 and the pressure measured by the QMS (GeneSys 300 by European Spectrometry Systems, dotted line). (c) Ratio between the signals given by a thermal conductivity gauge (Pirani PSG-101-S) and by a capacitive sensor (MKS Type 626A Baratron).

large batch (more than 700 vials) of lactose solution, with no empty vials as radiation shield, is considered. In Fig. 4.7a the temperature at the bottom of the product measured by a thermocouple inserted into a vial is shown. The water vapor concentration in the chamber, measured by a Panametrics moisture sensor, as well as the ratio between the signals given by a thermal conductivity gauge and by a capacitive sensor are shown in Fig. 4.7a and b, respectively; in Fig. 4.7b the measure given by a QMS, that is, the ionic current corresponding to the fragment of mass 18 divided by the total pressure reading made by the QMS, is shown. The response of the three devices is consistent and taking the point where the signal reaches a minimal and constant value as an estimate of the end of primary drying, a time of about 28–29 h results for all sensors. Actually, all the devices measure the concentration, or partial pressure, of water, even if adopting a different principle. As the chamber gas composition is dependent on the sublimation rate, and this is generally strongly reduced at the end of primary drying, a large variation in its value can be easily captured and used as an indication of the end of the sublimation step. However, it must be taken into account that this is an indirect measurement, affected by several variables, and problems can arise when changing the scale of the apparatus, the size of the batch, the method of pressure control in the chamber, or even the nature of the product. Better results can be obtained if the estimation of the sublimation flux is used to monitor the progress of the drying, as will be shown in the following (Pisano, 2009; Pisano *et al.*, 2009).

The shape of the curves obtained with the various devices is quite different. The moisture sensor shows quite a typical behavior: after the total pressure has been reduced to the operating value, the signal first sharply increases, and, after reaching a maximum, slowly decreases for almost all the primary drying, to drop towards the end. This behavior has already been described by Genin *et al.* (1996) who explained the slow decrease with the slight reduction in the drying rate due to increased thickness of the dry layer and, hence, of the mass transfer resistance, in the period of almost linear variation of residual ice thickness with time; the fast drop was explained by a large reduction in the sublimation rate. The moisture sensor was considered to be very sensitive by the first authors who studied it, being able to sense as few as 0.3% of the vials with ice remaining (Roy and Pikal, 1989): variation in the signal is large enough to detect the end of primary drying, but it suffers from low accuracy, that strongly limits the possibility of accurately estimating the amount of sublimed water from the integration of the moisture signal, and low response time. The latter is mainly due to water desorption from alumina, as noted by Genin *et al.* (1996) who reported that in the third phase the water desorption rate from the porous alumina could be an order of magnitude greater than desorption from the product at the beginning of secondary drying. The QMS requires a relatively long initial time interval for the stabilization of the pressure inside it; after that, the signal remains almost constant, until it drops, similarly to that of the moisture sensor. It can be concluded that, in the case of water solvent, the performance may be comparable to that of the moisture sensor, but it must be remembered that calibration is extremely difficult for QMS, the cost is much higher and operation requires caution. The use of the two pressure

gauges, if applicable, offers, in our opinion, the best compromise between cost and performance: the signal remains almost constant, until it starts to drop, and the use of the ratio of the two pressure signals, instead of a simple differential measure, allows a good sensitivity. The only inconvenience that has been observed is that the ratio of the signals of two pressure gauges can sometimes show a baseline signal shift at the end of primary drying, mainly due to the relatively low accuracy of the Pirani instrument that can make the determination of the end of sublimation uncertain. However, the decrease is initially very sharp and in very good agreement with the signals of the other devices.

The previous considerations may change if a third component is present in addition to inert and water, as in the case of the use of mixed solvents. In that case the response of the Pirani is affected by the presence of the new species, being unable to discriminate, even if the signal gets close to that of the capacitive gauge, when the composition of the chamber consists of only the inert species. The moisture sensor response, in principle, is independent of the presence of hydrocarbons, freon and carbon dioxide, but can be affected by low molecular weight alcohols, even if Roy and Pikal (1989) report having used it to monitor lyophilization of solutions containing up to 10% ethanol without any problems. The QMS in this case can obviously work efficiently and monitor the different species simultaneously.

In any case one must bear in mind that the response of all these devices can be biased by the fact that the atmosphere that they measure is not exactly the average one in the chamber and depends on the positioning of the sensor, on the use of controlled leakage and on the fluid dynamics of the vapor inside the chamber: the moisture sensor can be positioned properly in the chamber, but the movements of the shelf for the stoppering generally limit its use to a peripheral position, while the Pirani is connected to the chamber by a short duct and the QMS has to sample the gas from the chamber (Rasetto, 2009; Rasetto *et al.*, 2009).

Another sensor recently proposed to measure water concentration in the chamber is the cold plasma ionization device. The inductive coupled plasma/optical emission spectroscopy employs a radio-frequency that creates cold plasma in a quartz tube under vacuum; the light emitted by the plasma is characteristic of the gas present in the plasma. The optical spectrum is analyzed and a very sensitive measure of the humidity is displayed in real-time. The cold-plasma sensor seems particularly promising: it is steam sterilizable, simple to integrate even in an industrial-scale freeze-dryer, reproducible and sensitive; the main drawbacks are the uncertainty on the final point determination, the problem of calibration and the dependence of the response on the probe location (Mayeresse *et al.*, 2007). Figure 4.8 shows an example of the results that can be obtained by using the cold plasma sensor to monitor primary drying. As the vacuum was pulled down, the signal increased rapidly over 40 min to reach vapor saturation inside the freeze-drying chamber; it then remained saturated for about 12 h before decreasing according to a sigmoid-shaped curve. After 18 h of drying, the signal remained almost constant, thus indicating that most of the vapor had been replaced by nitrogen. After about 28 h secondary drying was started, with a shelf temperature rise and pressure drop: the sensor response detected this pressure drop and the baseline signal shifted to 8.5% of relative saturation.

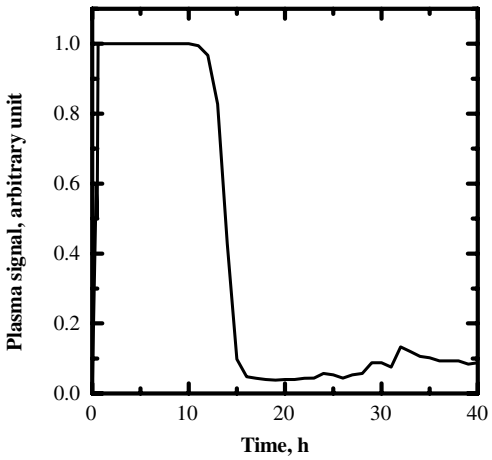

Fig. 4.8 Cold plasma sensor response during a freeze-drying cycle of 11000 vials with the sensor positioned on the top of the chamber (figure adapted from Mayeresse *et al.*, 2007).

Figure 4.9 shows a comparison of the results obtained during the freeze-drying of a 5% aqueous sucrose solution in plastic syringes (6 mm inner diameter) carried out at −40 °C and 26.6 Pa. Various devices are used to track the process, namely a Panametrics moisture analyzer, a Pirani gauge, a continuous weighing scale (manufactured by CHRIST) that provides a real time weighing under vacuum of a single product container (single syringe located inside the rack supporting the whole set of other containers or single vial placed on the shelf) and, finally, a LYOTRACK sensor (Adixen, France) that measures the humidity of the gas phase using the cold-plasma ionization principle (Hottot *et al.*, 2009).

Figure 4.9 shows that the sublimation end-point times derived from the CHRIST scale had always and systematically the lowest values (by about 3 h), in comparison with the other sensors, that presented comparable values (+/− 5%). The Pirani gauge and the LYOTRACK sensor showed similar humidity profiles, but significant noise was observed with the Pirani gauge signal, possibly due to air injection for total gas pressure regulation, whereas the LYOTRACK sensor was not disturbed at all by this air injection. Moreover, the Pirani gauge and the LYOTRACK sensor showed a saturation effect (with a nearly constant signal) about 300 min after the beginning of sublimation. It is also worth noting that the Panametrics hygrometer, which showed a continuously decreasing signal as a function of time, did not allow a clear sublimation end-point determination. Finally, Hottot *et al.* (2009) concluded that the LYOTRACK and Pirani sensors provided similar and consistent results, with clear and quite precise sublimation end-point determinations. Thus, the LYOTRACK sensor was recommended by these authors as being the more sensitive and the more precise sensor with a variation range between 100% and 1% (arbitrary units), instead of a variation range between 16 and 20 Pa in the case of the Pirani gauge. Moreover, this new sensor has the main advantages that it can be sterilized and it can be used with pure organic co-solvent formulations.

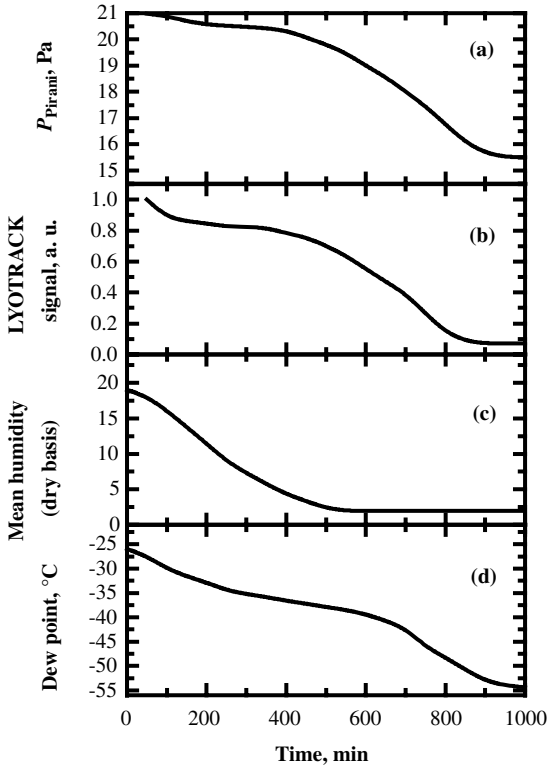

Fig. 4.9 Example of a freeze-drying cycle monitored using various devices: (a): Pirani gauge (filtered signal), (b) LYOTRACK sensor, (c) CHRIST scale, (d) Panametrics hygrometer. (Courtesy of Prof. J. Andrieu, LAGEP-CPE, Lyon, France).

Concerning the detection of the end of sublimation, as discussed above, it is generally assumed in previous works that it corresponds to the decrease of the monitored signal (e.g., pressure ratio or moisture concentration) to a low constant value, but it has been already pointed out that it may be difficult to define a respective numerical criterion, so that an uncertainty of a few hours can result. A significant difference in the value of the first derivative (end of plateau value), a zero value for the first derivative (end of the sharp signal decrease) or a zero value for the second derivative (inflection point in the middle of the sharp signal decrease) have been proposed as numerical criteria, but without a link to a theoretical background. In the case of the moisture sensor a special function called SEP(t) that uses the values of the total and partial pressure in the chamber and of the partial pressure in the condenser has been proposed on the basis of an inspectional analysis (Genin *et al.*, 1996). The exact determination of the endpoint with the previous type of sensors may be made intrinsically difficult by the fact that the desorption rate from the fraction of dried material and from the chamber walls can have a value comparable to the value of the sublimation rate at the end of the primary drying. One last comment concerns the duration of the period in which the signal drops; this is related to the heterogeneity of

the batch and to the process conditions, and can be quite long, for example, about 4–5 h in the case shown in Fig. 4.7 which refers to a relatively large batch where the side vials are affected by radiation. It must be stressed that the point where the signal starts decreasing with a large slope does not correspond to the point where all the vials have completed drying: in fact, Roy and Pikal (1989) have evidenced that the signal of the moisture sensor does not change slope even when a significant fraction of the vials have completed primary drying; these results have been confirmed by Pisano (2009) using the various sensors in some experiments carried out on a batch in which the heat flow was deliberately different for a fraction of the vials, stopping the cycle and measuring the residual water in the vials: when the Pirani-Baratron pressure ratio starts decreasing, a relevant fraction of vials of the batch are already dried in such a way that the flow rate is reduced under a critical value inducing a variation in the composition of the gas in the chamber.

4.3.3.2 **Monitoring the Primary Drying Using the Measurement of the Sublimation Flux**

A windmill sensor situated within the channel interconnecting the process chamber and the condenser has been proposed to monitor the batch: it can measure, at least qualitatively, the vapor flow, thereby providing information on the rate of freeze-drying, as well as on the completion of the freeze-drying processing (Tenedini and Bart, 2001). A different arrangement had been proposed by Couriel (1977), with a cover that fits over the tray and two turbines at either end of the tray: such a device would strongly limit the vapor flow, with negative effects on the product temperature, as discussed in the following.

The use of a mass flow controller to measure the gas flow necessary for pressure control and the tunable diode laser absorption spectroscopy sensor have been recently proposed to monitor the whole batch by means of direct or indirect measurement of the sublimation flow. When the pressure in the drying chamber is regulated by means of controlled leakage, the signal of the mass flow controller can be exploited to detect the end of the sublimation (Chase, 1998): in fact, the decrease in the partial pressure of water associated with the end of sublimation is responsible for the increase in the gas flow necessary to maintain a given chamber pressure. As an example, Fig. 4.10 shows the results obtained during the freeze-drying of 400 l of lactose in bulk: the nitrogen flow decreases sharply for approximately 2 h at the beginning of the operation as a consequence of the increase in the sublimation rate and the partial pressure of water as the lactose is heated. Over the following 13 h the nitrogen flow remains essentially constant, indicating relatively steady-state sublimation. The nitrogen flow starts to increase sharply after approximately 16 h of primary drying, as a consequence of the lower sublimation rate and, thus, of the reduction in the partial pressure of water in the chamber. During the next 2–3 h the nitrogen flow rate continues increasing until the slope decreases to zero, thus indicating that all the ice has sublimed and the chamber pressure is essentially made up of nitrogen gas.

The tunable diode laser absorption spectroscopy (TDLAS) sensor is a real-time, non-invasive device that is used to measure water vapor concentration and gas flow velocity in the duct connecting the freeze-drying chamber and the condenser using

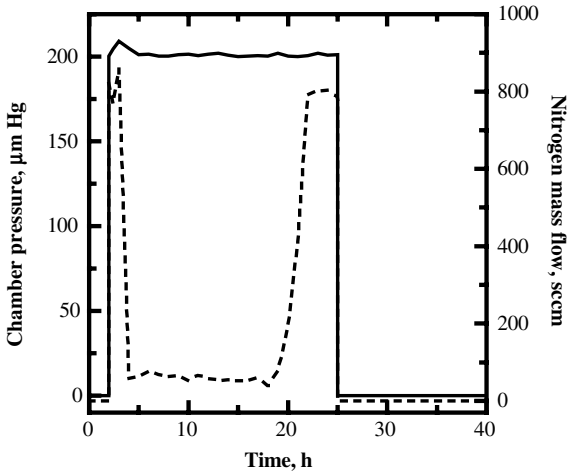

Fig. 4.10 Chamber pressure (solid line) and nitrogen flow (dashed line) during a freeze-drying cycle of 400 l of lactose in bulk (figure adapted from Chase, 1998).

Doppler-shifted near-infrared absorption spectroscopy (Kessler *et al.*, 2004; Gieseler *et al.*, 2007a). The concentration and gas velocity measurements are combined with knowledge of the duct cross-sectional area to determine the water vapor mass flow rate; the rate measurements can be integrated to provide a determination of the total water removed throughout the process. It has been proposed also for the determination of the heat transfer coefficient between the shelf and the product (Kuu *et al.*, 2009) and the temperature of the product (Schneid *et al.*, 2009): in both cases a mathematical model of the process is required to relate the sublimation flux measured by the TDLAS to the heat transfer coefficient (if the product temperature at the bottom of the vial is known) or to the product temperature (if the heat transfer coefficient is known). Moreover, because of its high sensitivity for residual moisture, the TDLAS sensor can be used to monitor secondary drying (Schneid *et al.*, 2007). This device can be installed in lab-scale and in production-scale equipment and can be easily placed in a sterile process environment, even if it could be difficult to retrofit existing units as it should be located in the freeze-dryer duct; the main drawbacks are the cost and the difficulty of calibration: fluid flow modeling can be used to provide acceptable density and velocity determinations (Kessler *et al.*, 2008).

The MTM-based methods, that also can provide information about the sublimation flux, will be discussed in the next section.

4.3.3.3 Monitoring the Primary Drying Using Methods Based on the PRT

Differently from the approaches previously discussed, methods based on the pressure rise test are able to give information about the state of the whole system, that is, the temperature and the residual water content, and can thus be used in a control loop; in addition, they also allow evaluation of the sublimation rate and, thus, the same considerations discussed above hold, even if the information can be obtained only at discrete times. Early works (Neumann, 1961, 1986; Nail and

Johnson, 1991; Willemer, 1991) investigated the transient pressure response measured during a PRT, using it as a method for determining the end of primary drying, or for an estimate of the product temperature based on the saturating steam pressure of the ice. Oetjen proposed and patented a method, called barometric temperature measurement (BTM), to estimate the temperature of the subliming interface using the value of the pressure at which the first derivative of the pressure rise curve has a maximum (Oetjen, 1999; Oetjen *et al.*, 2000; Oetjen and Haseley, 2004). Mathematical models have been used in the past to compute the temperature of products undergoing lyophilization on the basis of pressure rise data (Milton *et al.*, 1997; Liapis and Sadikoglu, 1998; Obert, 2001; Chouvenc *et al.*, 2004; Velardi *et al.*, 2008). In all these algorithms some parameters of the system are calculated by means of a regression analysis, that is, by fitting the measured pressure rise response to the values calculated using a mathematical model: what differentiates one method from the others is the mathematical model and the parameters estimated.

Milton *et al.* (1997) proposed the manometric temperature measurement (MTM): the transient pressure response is mathematically modeled under the assumption that four mechanisms contribute to the pressure rise, namely the direct sublimation of ice through the dried product layer at a constant temperature, the increase in the ice temperature due to continuous heating of the frozen matrix during the measurement, the increase in the temperature at the sublimation interface when a stationary temperature profile is obtained in the frozen layer and, finally, the leaks in the chamber. The four contributions are considered purely additive; the values of the thickness and of the thermal gradient are needed but they are not known exactly. The values of the vapor pressure over ice, of the product resistance and the heat transfer coefficient at the vial bottom are determined with regression analysis.

A modification of the previous model was proposed by Obert (2001) who considered also the desorption of the bound water during the primary drying, which can contribute to the increase in the total pressure, and the thermal inertia of the glass wall of the vial. The temperature at the bottom of the vial and the thickness of the frozen layer should be known in order to use this algorithm, but they are only guessed in the proposed procedure. The overall heat transfer coefficient is expressed adopting the heat and mass transfer steady-state hypothesis, while a non-linear regression analysis is carried out in order to estimate the vapor pressure at the interface, the mass transfer resistance in the dried product and the desorption rate.

A more rigorous model, based on heat and mass balances, is used in the pressure rise analysis (PRA) proposed by Chouvenc *et al.* (2004). The thermal capacity of the portion of the vial glass in contact with the frozen product is taken into account in the heat balance for the frozen product. They assume that the temperature increase at the interface is the same as the mean product temperature rise, which would be exact if the temperature gradient along the ice during the PRT were constant. This assumption can be reasonable towards the end of the primary drying, when the thickness of the ice is small, but not in the first part of the drying cycle, when the frozen layer thickness is higher and accumulation effects prevent the temperature gradient from being constant. Chouvenc *et al.* (2004) also assume a constant temperature at the vial bottom during the PRT; however, the vial bottom is

continuously heated during the process, while the heat removal at the interface is reduced due to the increased chamber pressure, which reduces the driving force for sublimation. The thickness of the frozen layer is estimated by considering constant sublimation flow between two subsequent PRTs: the value of the thickness in a generic run is retrieved by subtracting from the total initial mass of product the sum of the mass sublimed up to the time of the current PRT. The subliming interface temperature at the beginning of the PRT and the mass transfer resistance of the porous layer are estimated through regression.

A more complex mathematical model (Sadikoglu and Liapis, 1997) has been used by Liapis and Sadikoglu (1998) to estimate the whole temperature profile in the frozen layer of the product and the position of the moving front. Many parameters are needed to perform the analysis, namely the diffusivity and the permeability of the porous layer, the shelf-vial heat transfer coefficient, the temperature and the partial pressure at the top of the vial, thus making its practical in-line application a complex task, even if feasible in theory.

The dynamic parameters estimation (DPE) algorithm proposed by Velardi *et al.* (2008) solves the energy balance for the frozen layer to get the temperature profile in the product taking into account the different dynamics of the temperature at the interface and at the vial bottom. The energy balance in the frozen layer during the PRT can be described by the following equations:

$$\frac{\partial T}{\partial t} = \frac{\lambda_{\text{frozen}}}{\varrho_{\text{frozen}} c_{\text{p,frozen}}} \frac{\partial^2 T}{\partial z^2} \quad \text{for} \quad t > t_0,\ 0 \le z \le L_{\text{frozen}} \tag{4.4}$$

$$T|_{t=t_0} = T_{\text{i},0} + \frac{z}{\lambda_{\text{frozen}}} \Delta h_{\text{s}} \frac{K\tilde{M}_{\text{w}}}{\tilde{R}T_{\text{i},0}} \frac{p_{\text{w,i},0} - p_{\text{w,c},0}}{L - L_{\text{frozen}}} \quad \text{for} \quad 0 \le z \le L_{\text{frozen}} \tag{4.5}$$

$$\lambda_{\text{frozen}} \frac{\partial T}{\partial z}\bigg|_{z=0} = \Delta h_{\text{s}} \frac{K\tilde{M}_{\text{w}}}{\tilde{R}T_{\text{i}}} \frac{p_{\text{w,i}} - p_{\text{w,c}}}{L - L_{\text{frozen}}} \quad \text{for} \quad t \ge t_0 \tag{4.6}$$

$$\lambda_{\text{frozen}} \frac{\partial T}{\partial z}\bigg|_{z=L_{\text{frozen}}} = K_{\text{v}}(T_{\text{shelf}} - T_{\text{B}}) \quad \text{for} \quad t \ge t_0 \tag{4.7}$$

Thermodynamic equilibrium is assumed at the subliming interface; moreover, at the beginning of the PRT the heat fluxes at $z = 0$ (interface) and at $z = L_{\text{frozen}}$ (bottom of the vial) are assumed to be equal, thus K_{v} can be derived by equating the boundary conditions from Eqs. 4.6 and 4.7, both taken at $t = t_0$:

$$K_{\text{v}} = \left[\frac{T_{\text{shelf}} - T_{\text{i},0}}{\Delta h_{\text{s}} \frac{K\tilde{M}_{\text{w}}}{\tilde{R}T_{\text{i},0}} \frac{p_{\text{w,i},0} - p_{\text{w,c},0}}{L - L_{\text{frozen}}}} - \frac{L_{\text{frozen}}}{\lambda_{\text{frozen}}} \right]^{-1} \tag{4.8}$$

Figure 4.11a shows a sketch of the vial geometry with the coordinate system.

Due to the contribution of gas conduction, K_{v} is dependent on the pressure, which varies during the PRT, but, as has been evidenced by Chouvenc *et al.* (2004), due to the thermal inertia of the system this dependence is not relevant during the PRT and the constant value given by Eq. 4.8 can be used. The radiation flux from the bottom is accounted for in the overall heat transfer coefficient that is estimated from numerical

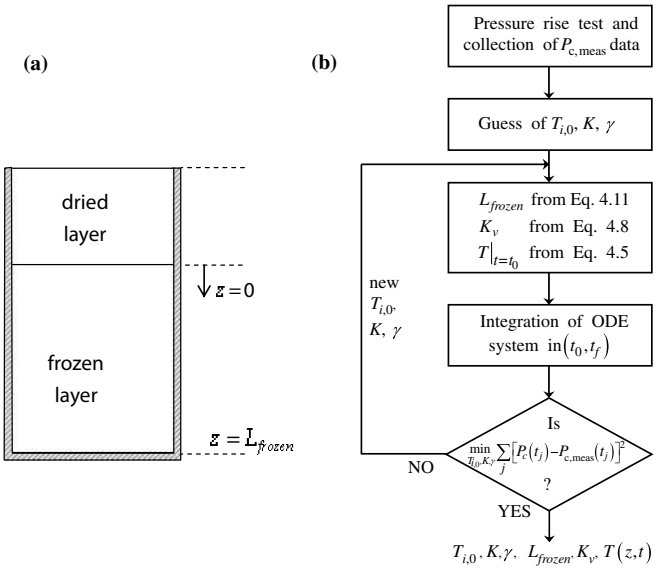

Fig. 4.11 (a) sketch of the vial geometry with the coordinate system used by the DPE algorithm and (b) steps of the optimization procedure in the DPE algorithm.

regression. Radiation from the upper tray generally has a negligible effect due to the presence of the stopper that, at least partially, shields the product, and of the dried layer. Radiation from the side-walls affects the dynamics of a very low number of vials (only 6–7% of the vials of a batch in an industrial-scale apparatus are affected by radiation, that is, those placed at the side of the shelf) while in a small-scale apparatus, used for R&D purposes, the problem should be avoided by proper shielding; anyway, a small radiative contribution to total heat transfer is not a problem and, as long as the shape of the axial temperature profile is not significantly modified, the interface temperature is still predicted with good accuracy and the radiation has only the effect of increasing the value of the estimated effective heat transfer coefficient. Concerning the role of the vial wall in the thermal balance of the system, it can be relevant during the primary drying (Schelenz *et al.*, 1994; Brülls and Rasmuson, 2002; Hottot *et al.*, 2006; Velardi and Barresi, 2008a). Nevertheless, it has been proven that the effect of the vial wall, with respect to the heat conduction in the axial direction and to the radiative flux from the chamber wall, can be accounted for in a one-dimensional model by using an effective heat transfer coefficient (Velardi and Barresi, 2008a). Moreover, the contribution of the vial wall to the dynamics of the system during the PRT has been shown, by means of numerical simulations, to be negligible and, for this reason, it has not been considered in the DPE algorithm, differently from Chouvenc *et al.* (2004) who included in the lumped model a fraction of the heat capacity of the glass to be determined by fitting (Fissore *et al.*, 2011a).

The total pressure is calculated taking into account a constant leakage in the chamber:

$$P_c = p_w + p_{in} = p_w + F_{leak}t + p_{in,0} \quad \text{for} \quad t \geq t_0 \tag{4.9}$$

Applying the ideal gas law and rewriting the mass flow rate as function of the pressure driving force between the interface and the chamber, it follows that:

$$\frac{\tilde{M}_w V_c}{\tilde{R} T_c} \frac{dp_{w,c}}{dt} = N_v A \frac{K \tilde{M}_w}{\tilde{R} T_i} \frac{p_{w,i} - p_{w,c}}{L - L_{frozen}} \quad \text{for} \quad t \geq t_0 \tag{4.10}$$

Equation 4.10 is valid if the contribution of all the vials is the same, that is, all the vials have the same values of L, T_i, K. Nevertheless, due to water vapor hydrodynamics and radiation effects the batch can be inhomogeneous (Barresi *et al.*, 2008a, b): as an example, vials located at the edge of the plate sublime faster due to radiation from the wall. As a consequence, when in some vials the primary drying is completed, in other vials the main drying is still taking place and thus the number of vials contributing to the pressure rise during the PRT is different from N_v. For this reason it is generally assumed that methods based on the PRT give accurate and coherent data only in the first half of the primary drying (see, for example, Hottot *et al.*, 2005; Tang *et al.*, 2005), as at the end of this step a fraction of the vials can have completed sublimation before the rest of the batch. To take into account this effect, the term $N_v A$ in Eq. 4.10 can be multiplied by a parameter, γ, that is equal to one at the beginning of primary drying and that decreases during drying (Rasetto *et al.*, 2008): the value of this parameter can be estimated by means of the DPE algorithm or it can be calculated independently (Barresi *et al.*, 2010).

If the value of the gas temperature in the chamber, T_c, is not available, it can be substituted with the product temperature at the interface with a negligible error. The actual thickness of the frozen layer is calculated from a mass balance written across the moving interface, which is solved with the previous equations. This balance can be integrated in time, using for example the trapezoidal rule of integration, between the previous PRT and the actual one, thus obtaining:

$$L_{frozen} = L_{frozen}^{(-1)} - \frac{\tilde{M}_w}{\tilde{R} \Delta \varrho} \left[\frac{K}{T_{i,0}} \frac{p_{w,i,0} - p_{w,c,0}}{L - L_{frozen}} + \frac{K^{(-1)}}{T_{i,0}^{(-1)}} \frac{p_{w,i,0}^{(-1)} - p_{w,c,0}^{(-1)}}{L - L_{frozen}^{(-1)}} \right] \frac{t_0 - t_0^{(-1)}}{2} \tag{4.11}$$

where $\Delta \varrho = \varrho_{frozen} - \varrho_{dried}$ and the superscript "(-1)" refers to quantities calculated or measured in the previous PRT.

The steps of the DPE algorithm are summarized in Fig. 4.11b. In previous equations, and in particular in Eqs. 4.5 and 4.6, the gas flow rate in the dried layer was calculated including the dependence on cake thickness, but neglecting the resistance of the stopper. As an alternative the global mass transfer resistance, R_p, can be used:

$$\frac{1}{R_p} = \frac{\tilde{M}_w}{\tilde{R} T_i} \frac{K}{L - L_{frozen}} \tag{4.12}$$

If the stopper resistance is not negligible, then the global resistance to vapor flow in the dried layer is given by:

$$\frac{1}{R_p + R_s} = \left(\frac{\tilde{R} T_i}{\tilde{M}_w} \frac{L - L_{frozen}}{K} + R_s \right)^{-1} \tag{4.13}$$

The DPE algorithm has been demonstrated to work efficiently both under heat transfer and mass transfer control (Barresi *et al.*, 2009c) as it estimates both the heat transfer coefficient and the resistance to the mass flow. This is an advantage with respect to other approaches proposed in the literature which require one to assess if the system is under heat or mass transfer control (Liapis and Litchfield, 1979; Litchfield and Liapis, 1982).

If the valve used to separate the drying chamber from the condenser during the PRT is fast closing, as is generally the case in medium and small scale equipment, its dynamics can be neglected; anyway, it has been shown that a slow dynamics can be accounted for in the algorithms based on the PRT (Oetjen and Haseley, 2004; Chouvenc *et al.*, 2005). As an example, Chouvenc *et al.* (2005) assumed that part of the flux generated by sublimation of ice and, eventually, to a lesser extent, by the chamber leak rate of inert gas, is lost, during the transient closing period; this fraction is considered variable with time, in the time interval required to get the valve fully closed, and is a characteristic of the isolation valve and independent of the operating conditions. This valve characteristic function was then taken into account in the PRA algorithm.

The sensitivity of the methods based on the PRT depends on the chamber volume and on the sensitivity of the pressure gauge, in addition to the operating conditions and the nature of the product that influences the value of the sublimation rate. According to the literature (Milton *et al.*, 1997), the sensitivity depends on the ratio of the active subliming surface area to the chamber volume and it decreases as the batch size decreases. Milton *et al.* (1997) do not specify any lower bound needed to get reliable data. In this context, it may be noted that in production apparatus the most sensitive capacitive gauge available is generally used, with a full scale of only 100 Pa, while in lab-scale freeze-dryers often a gauge with larger scale is used. Milton *et al.* (1997) carried out their measurements successfully with a value of the chamber volume to the subliming surface area corresponding to 1.28 m; Tang *et al.* (2006b) and Gieseler *et al.* (2007b) reported that in order to get accurate temperature measurement using the MTM algorithm a value not higher than 3.5 m was required. We were able to carry out PRTs even with a very small number of vials, up to a chamber volume to subliming surface area ratio of 58 m that corresponds, for the cases investigated, to a sublimation flow/chamber volume ratio (the parameter we suggest to consider) equal to 1.4×10^{-2} kg h^{-1} m^{-3} (Pisano, 2009).

Figure 4.12 shows a comparison between the temperature of the product at the bottom of the vials estimated by DPE, MTM and PRA (assuming $\gamma = 1$); the values of the shelf temperature and of the temperatures measured by some thermocouples are also shown in the upper graph, as well as the ratio of the signal of the Baratron and of the Pirani gauges. One point to be evidenced is that, generally, the estimated product temperature decreases near the end-point, but this drop may be only an artifact because a fraction of vials, the edge-vials, has already finished subliming while DPE,

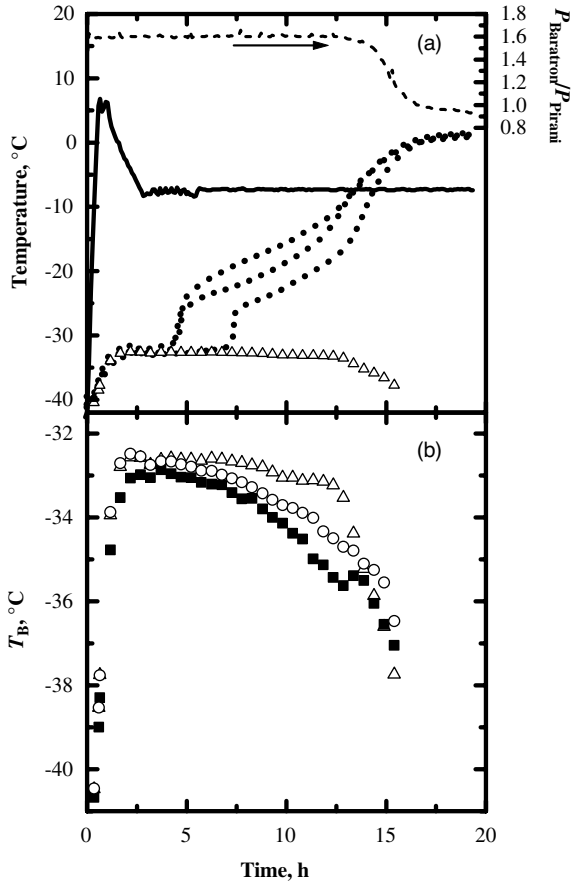

Fig. 4.12 Monitoring of the freeze-drying cycle of 10% by weight sucrose solution ($N_v = 175$, $d_v = 14.2 \times 10^{-3}$ m, $L_p = 7.2 \times 10^{-3}$ m, $P_c = 10$ Pa). (a) Comparison between bottom product temperature estimated by DPE (△) and the values measured by thermocouples in close contact with the bottom of the vial (dotted lines). The heating fluid temperature (solid line) and the Pirani to Baratron pressure ratio (dashed line) are also shown. (b) Comparison between the predictions of the temperature at the bottom of the vial obtained using various algorithms (■: MTM, ○: PRA, △: DPE with $\gamma = 1$).

MTM and PRA continue interpreting pressure rise curves assuming batch uniformity, or rather a constant number of subliming vials. Thus, a decrease in pressure rise, corresponding to a lower sublimation rate, may be interpreted by these algorithms as a reduction in the front temperature. From comparison of these methods it is possible to see that the estimations provided by MTM are reliable only in the first half of the primary drying, after which the estimated temperature exhibits a strong decrease, while the estimations of DPE, that uses a much more complex model to describe the pressure rise occurring during a PRT, are consistent for a larger fraction of the primary drying.

The decrease in the interface temperature estimated by these methods based on the PRT was already reported by Oetjen and Haseley (2004), who proposed to use it as an indication of the end of sublimation; according to the results shown this is not correct, or at least should be interpreted as an indication of the end of the sublimation in the first vials, but in our opinion this criterion is not very robust. Moreover, recent preliminary results show that batch heterogeneity is surely responsible, at least partly, for the observed behavior, but this can also be due to the optimization algorithm and caused by problem ill-conditioning (Fissore *et al.*, 2011a). Anyway, the end of primary drying could be reasonably estimated by extrapolating the predictions of the interface position obtained in the initial part of the run. The estimation of the solvent flux can be used as an alternative way to detect the endpoint of the primary drying: when the solvent flux decreases below a specific limit the main drying can be considered finished. As discussed above, various approaches can be used to obtain estimations of the sublimation flux, for example, the slope of the curve of the pressure rise at the beginning of the PRT, a balance inserted in the drying chamber, the DPE, a system like the TDLAS or the mass flow of nitrogen in the case of controlled leakage. Nevertheless, a decrease in the fluid temperature, and thus in the heat flux given to the system, can also decrease the solvent flux, so that this information has to be coupled with other measurements to assess the end of primary drying: if product temperature is approaching the shelf temperature, then primary drying can be considered completed.

Recently, an integrated criterion was proposed to estimate the end of the primary drying: DPE is used to estimate the sublimation flux, and the actual mass of sublimed solvent and the frozen layer thickness are calculated after each PRT by integration of the flux over time; the average mass sublimation rate is then calculated and when this is lower than a fixed bound, the primary drying is considered completely finished (Velardi and Barresi, 2008b; Pisano, 2009; Pisano *et al.*, 2009, 2010a). The steps of the algorithm are the following:

- Do a PRT and run the DPE algorithm to obtain a full estimation of the state of the system in terms of product temperature and heat and mass transfer coefficients.
- Calculate the current solvent flux using either DPE outcomes or the slope of the pressure rise curve at the beginning of the test.
- Integrate the solvent flow rate over time so as to calculate the current sublimed mass of solvent.
- Calculate a stop coefficient that is directly related to the average subliming mass rate and is used as a reference for establishing whether or not the main drying is finished:

$$C = \frac{m(t_i) - m(t_{i\text{-}1})}{t_i - t_{i\text{-}1}} \frac{1}{m_{tot}} \tag{4.14}$$

where t_i is the current time instant and t_{i-1} is the time instant at which the previous PRT was done.

- Compare this coefficient with a lower bound fixed by the user, which consists in the percentage variation of the sublimed solvent mass with respect to the total one

(for example 1% h^{-1}). If C is lower than this limit and the estimated frozen layer thickness is not close to the initial one, confirming that the process is not at the beginning, when the sublimation rate can be low due to the low initial product temperature, the primary drying can be considered finished.

- If the sublimation step is not yet finished, it could be interesting to estimate the time left to the endpoint. This can be easily done using a mathematical model that describes the dynamics of the process (e.g., the same as in the DPE algorithm) and uses the process parameters estimated by DPE.

Figure 4.13 compares the endpoint time estimated using the previously described algorithm and other devices. The cycle has been run loading in the freeze-dryer only the 15 vials monitored by the balance, thus avoiding any difference between the dynamics of the vials of the balance and that of others of the batch. We can see that there is very good agreement between the flow rate measured by mass measurements and by the pressure rise technique. On the contrary, it can be noticed that the product temperature response detected the end of the two monitored vials 10 h before the real endpoint, which can be explained by a higher drying rate of the vials wherein the thermocouple probe is inserted. The endpoint time, equal to 18.5 h, agrees with the

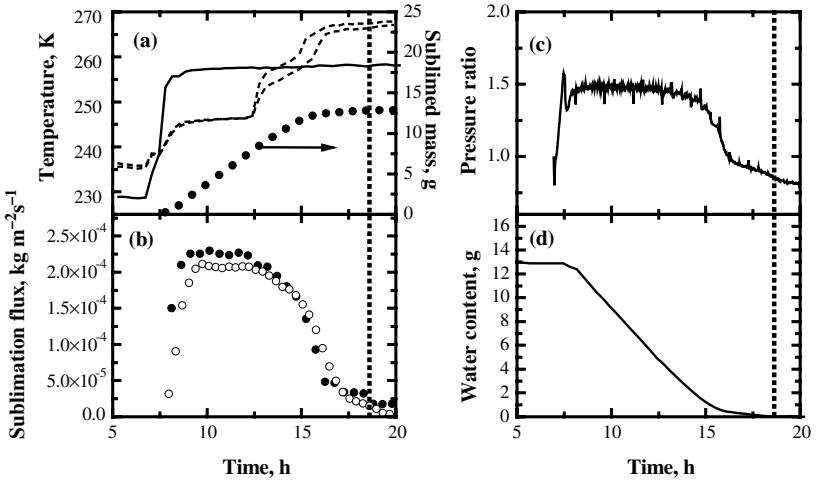

Fig. 4.13 Example of the results obtained during a freeze-drying cycle using various devices to track the primary drying stage of 10% by weight sucrose solution in a pilot-scale freeze-dryer. The freezing phase was run at 223 K for about 5 h, while during the primary drying phase the fluid temperature was set at 253 K and the chamber pressure at 10 Pa ($N_v = 15$, $d_v = 14.2 \times 10^{-3}$ m, $L_p = 7.2 \times 10^{-3}$ m, not shielded). (a) Comparison between the endpoint time evaluated by means of the algorithm described in the text (vertical dotted line) and the product temperature response (dashed lines); the shelf temperature (solid line) and the sublimed solvent mass evolution calculated by integration of the flux estimated from the slope of the pressure rise curve (symbols) are also reported. (b) Comparison between the ice sublimation flux calculated from the pressure rise curves (●) and from the mass measurements (○). (c) Pirani–Baratron pressure ratio. (d) Evolution of the water mass left in the 15 monitored vials measured by the balance.

value measured by both the Pirani–Baratron pressure ratio and product mass evolution.

From the previous discussion it becomes evident that various devices should be used together to monitor primary drying. The *LyoMonitor* (Barresi *et al.*, 2009a) is an example of a system that can manage various devices and collect their measurements to monitor primary drying. Currently, as shown in Fig. 4.14, it includes various sensors, namely:

- A multi-point wired thermometer composed of a set of nine copper–constantan thermocouples, a conditioning circuit and a commercial multimeter equipped with a multiplexer.
- An innovative wireless thermometer (Vallan *et al.*, 2005a) that can manage one or more measurement modules equipped with 14 thermocouples each: it sends the results to a "reader" placed outside the vacuum chamber and connected by means of a serial interface to a PC that schedules, acquires and collects the measurements. The reader powers the thermometer and the modules through the same radio-frequency link that is employed for data communication, so that the modules can work without batteries.
- A special weighing device (Vallan *et al.*, 2005b; Vallan, 2007) working inside the vacuum chamber and able to measure contemporaneously the weight and temperature of a group of vials during the drying process (see Section 4.3.2).
- A valve control and an acquisition system for the PRT.
- Pressure and moisture sensors: the system is able to acquire the output signal of a thermal conductivity gauge, a capacitance manometer and a moisture analyzer by means of an external multimeter that is interfaced to the PC through the IEEE-488 interface.

Moreover, some other process variables that are measured in the freeze-dryer using embedded devices (i.e., shelf and fluid temperatures, controlled-leakage valve opening and inert mass flow rate for pressure control) can be acquired through a dedicated RS485 interface, thus providing a complete evaluation of the status of the system.

A monitoring system like *LyoMonitor* allows one to monitor both single vials, using the soft-sensor, as well as the whole batch, using the PRT and the DPE algorithm. Moreover, the soft-sensor can be coupled to the DPE algorithm: the values of the interface temperature, of the heat transfer coefficient between the fluid and the bottom product and of the mass transfer resistance in the dried layer estimated by the DPE algorithm can be used to initialize the equations of the observer as this strongly improves the convergence of the algorithm of the observer (Barresi *et al.*, 2009c). DPE and soft-sensor give similar information about the state of the product, but it hardly happens that the values they provide are the same: data reconciliation is thus required. As far as the detection of the ending point of primary drying is concerned, *LyoMonitor* allows one to track various signals, that is, the Pirani–Baratron ratio, the reading of the moisture analyzer, the measurement of the weight loss of a group of vials, the estimation of the sublimation flux obtained by means of DPE and the residual ice content given by the soft-sensor. As previously

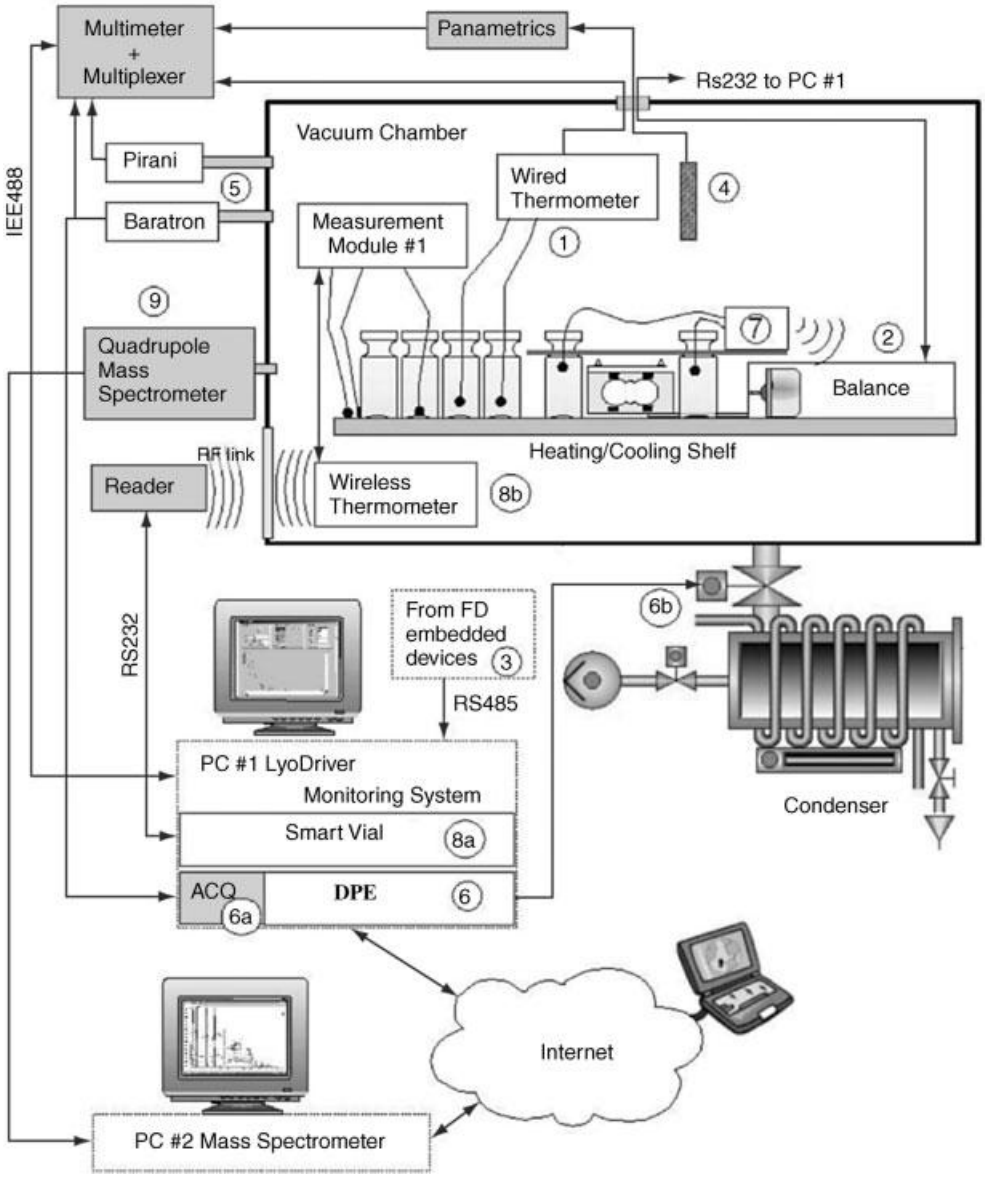

Fig. 4.14 Scheme of the *LyoMonitor* system: (1) multi-point thermometer equipped with fault diagnosis for product and chamber monitoring; (2) proprietary in-line balance; (3) signal acquisition from embedded devices; (4) capacitive moisture sensor; (5) pressure sensors: capacitance manometer and thermal conductivity gauge; (6) "dynamic parameters estimation" (DPE) with fast pressure data acquisition through an acquisition board (6a) and valve control for pressure rise test (6b); (7) miniaturized radio-controlled thermometer for the vials weighed by the balance; (8) "smart vial" observer (8a) and wireless additional thermometer (8b); (9) QMS.

discussed, all these signals can be used to detect the end of the primary drying, with some limitations, and thus the user should carefully monitor all of them in order to assess the end of this stage.

4.4
Control of the Primary Drying

As stated in the introduction, the control of a freeze-drying process, with the goal to reduce the time required to reach the desired amount of residual solvent, is a challenging task due to the impossibility of measuring in-line the variables of interest, that is, the product temperature and the residual solvent content.

Some papers have appeared in the past about this issue and proposed to use a mathematical model of the process to calculate off-line the optimal operating conditions (i.e., the shelf temperature and the chamber pressure) for the primary drying. A very simple approach consists of carrying out the process using constant values for the chamber pressure and for the temperature of the heating shelf: Fig. 4.15 shows an example of the results that can be obtained using the detailed one-dimensional model of Velardi and Barresi (2008a) to calculate the time required to

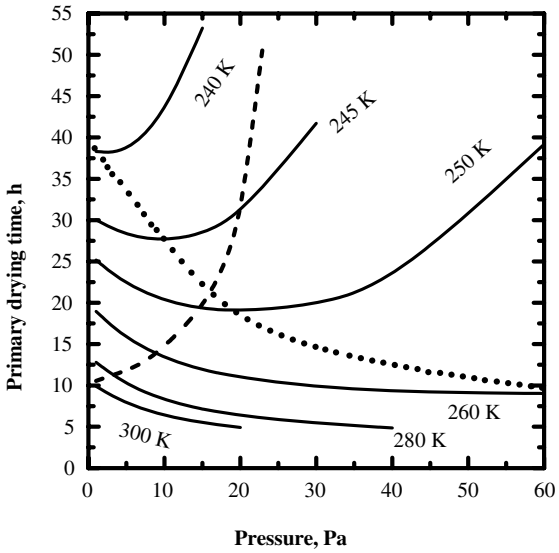

Fig. 4.15 Effect of chamber pressure and heating shelf temperature on the primary drying time for constant shelf temperature. The locus corresponding to the minimum of the primary drying time for the various shelf temperatures is also shown (dotted line). The dashed line corresponds to the values of chamber pressure and of shelf temperature that satisfy the constraint on the maximum product temperature. Case study: 5% solution of Bovine Serum Albumin solution (Fissore *et al.*, 2008a).

complete the primary drying in a vial placed at the center of the shelf, for which radiation can be neglected.

For a given T_{shelf} it is possible to find an optimum value of the chamber pressure that minimizes the drying time. In fact, when operating at very low vacuum, a pressure increase leads to a diminution of the drying time because heat transfer is improved; however, if the pressure is raised beyond a certain value, the time required to complete the primary drying starts to increase because the driving force for mass transfer becomes too small and sublimation takes place slowly. The optimum condition is visible in Fig. 4.15 (dotted line) for the curves calculated using values of T_{shelf} lower than 260 K, while it is shifted to pressures higher than 60 Pa if T_{shelf} is higher than 260 K. The calculated couple of values of T_{shelf} and of chamber pressure that minimize the primary drying step does not take into account the presence of the constraint given by the maximum temperature that allows safe operation without any denaturation of the product. If the maximum product temperature is taken into account (240 K in this example) the optimal pressure becomes, in this case, the minimum that can be obtained in the apparatus (dashed line).

Some advantages can be obtained if the operation is carried out with a shelf temperature and a chamber pressure that vary during the operation. Liapis and Litchfield (1979) used a quasi-steady-state model of the process to optimize the primary drying; constraints are placed on the scorch temperature of the dried product and on the melting point of the frozen product. As the temperature profile in the vial is fully known from the mathematical simulation of the process, they distinguish between a process whose dynamics is controlled by the heat transfer from the shelf and a process whose dynamics is controlled by the mass transfer: in the first case the manipulation of the shelf temperature is effective, while in the second case it is necessary to manipulate the chamber pressure. A similar approach has been used by Lombraña and Diaz (1987a, b), while variational calculus involving a detailed multidimensional model of the process has been used by Sadikoglu *et al.* (2003). Fissore *et al.* (2008a) proposed to continuously manipulate the shelf temperature so that the maximum product temperature ($T_{p,max}$) is equal to the maximum allowable value ($T^*_{p,max}$) at any instant. The control law is thus expressed as:

$$T_{shelf}(t) = f(T_{p,max}, t) \tag{4.15}$$

A mathematical model of the process is required to link the shelf temperature to the maximum product temperature. An example of the results that can be obtained using this control algorithm is given in Fig. 4.16a. At the beginning of the drying phase T_{shelf} is raised at a 0.5 K min^{-1} constant rate; after about 2 h of drying, when the shelf temperature reaches a value of 281 K, the product temperature becomes equal to the maximum allowed value (240 K) and the control logic overrides the initial heating program (solid lines): the temperature of the shelf starts being regulated in such a way that $T_{p,max}$ remains constant and equal to the target value. In this way the primary drying is completed in 13.5 h, as can be seen from the time evolution of the position of the sublimation front (Fig. 4.16b). If the shelf temperature is maintained constant, the product temperature is left free to vary (dashed lines); thus, T_{shelf} must be fixed at a

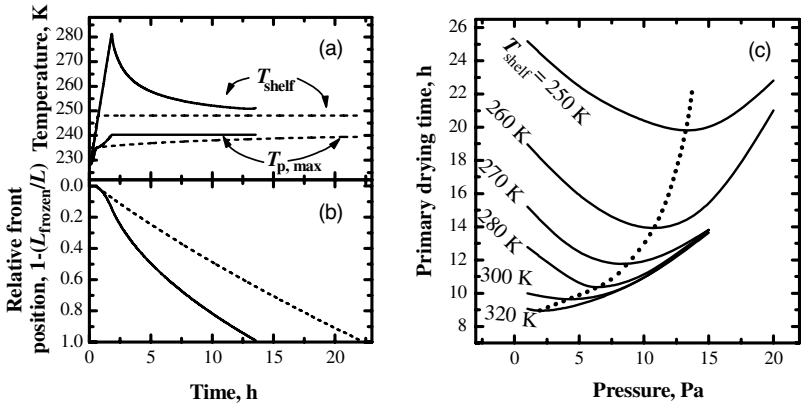

Fig. 4.16 (a) and (b) Comparison between the model-based control strategy (solid lines) and the constant T_{shelf} (dashed lines) for the freeze-drying of a 5% solution of Bovine Serum Albumin ($d_v = 14.2 \times 10^{-3}$ m, $L_p = 8 \times 10^{-3}$ m, $P_c = 15$ Pa, $T^*_{p,max} = 240$ K). (a) Time evolution of the temperature of the heating shelf and of the maximum temperature of the product; (b) moving front position. (c) Effect of chamber pressure and heating shelf temperature on the primary drying time when the process is controlled using the model-based control strategy that maintains the maximum product temperature at a value lower than 240 K. The locus corresponding to the minimum of the primary drying time for the various shelf temperatures is also shown (dotted line). Case study: 5% solution of Bovine Serum Albumin (Fissore *et al.*, 2008a).

lower value in order not to exceed the maximum allowed temperature that is approached only at the end of the drying phase: a longer primary drying time is thus obtained (the moving front reaches the bottom of the vial after 22 h). Various simulations of the primary drying can be carried out for different values of the pressure in the chamber and using the previously described control strategy: results are given in Fig. 4.16c. In these simulations T_{shelf} is initially ramped at 0.5 K min^{-1} to the set-point value of T_{shelf}, which parametrizes the curves. Then T_{shelf} is maintained constant until the maximum product temperature reaches the respective limiting value (set equal to 240 K in this example). At this point the previously described control strategy takes over. It is possible to identify also in this case a curve (dotted line) which represents the locus of the values of chamber pressure and initial set-point of T_{shelf} that ensure minimization of the time required to complete the primary drying and to compare this locus with the analogous one obtained in the case of constant T_{shelf}. For example, if T_{shelf} is maintained constant at 280 K and the constraint on the maximum product temperature is active, the minimum drying time (11.1 h) is obtained at a pressure of 3.3 Pa, while, when the optimal heat input strategy is adopted, a lower minimum drying time is found (10.25 h) with a higher chamber pressure (6.75 Pa), thus with minor energy consumption. Concerning the case of constant shelf temperature (Fig. 4.15), it can be observed that the best operating conditions are those with $T_{shelf} \cong 300$ K and with a value of the chamber pressure as low as possible, resulting in a minimum time of 10.5 h. In the case of a variable heating strategy, the pressure should also be as low as possible, but with an

initial set-point $T_{shelf} \cong 320\,K$ the main drying ends after 9 h. Thus, it can be concluded that the manipulation of T_{shelf} allows one to carry out the process faster, under the constraint given by the maximum allowable temperature of the product. Chamber pressure is maintained constant: it is varied in the case of emergency, when, due to errors in the off-line optimization or to malfunctioning of the control system, the maximum temperature of the product increases beyond the limit value. In such a situation pulling the vacuum down immediately works as a thermal switch with an instantaneous result, whereas cooling the shelves requires a longer time (Rey and May, 2004).

The main drawback of all these model-based algorithms is that they require that the model describes perfectly the dynamics of the process and that all the parameters and all the variables of the process are known. As this seldom happens, it is necessary to use one of the techniques described in Section 4.3 to monitor the primary drying in order to know the value of the temperature of the product, that is the controlled variable, and, thus, to calculate the control action.

The first automatic control systems proposed date back to the early 1960s, and were based either on the barometric temperature measurement of the batch or on the monitoring of the resistivity of one or more sampled vials. Even if they had many limitations, and up to recent times were never really applied in industrial applications, especially those of the second kind, they introduced the concept of modern closed-loop control, and some control strategies that are still valid (Nail and Gatlin, 1985; Jennings, 1999).

Thus Rey (1963, 1976) proposed to manipulate the shelf temperature to maintain constant resistivity, measuring eventually more vials to take into account non-homogeneity of the batch. An improved monitoring method, based on the resistivity measurement of the sample and of a comparison material, together with the product temperature, was proposed by Jennings (1982) to increase product yield. Rieutord (1965) also proposed to use the resistivity measurement as an alternative to temperature measurement, but showed that by acting on the total pressure in the drying enclosure it was possible to supervise and regulate the energy supply to the product: to this end he realized the controlled bleeding system, using an inert gas to control the pressure in the chamber; the shelf temperature could be kept constant, or regulated independently. The possibility of independent temperature control of the different shelves was also considered. The manipulation of shelf temperature and chamber pressure for control of heat transfer have very different performances: the first one is slow and unstable, as a consequence of the large lag compared to the fast response of resistivity, while direct control of inert gas flow is more rapid, but does not inherently balance the heat transfer rates. Jefferis (1981, 1983) elaborated a cascade control algorithm in which dryer pressure was a function of product resistivity and condenser temperature.

A simple control system for the shelf temperature based on the BTM output was first proposed by Neumann (1961) and then described by Oetjen *et al.* (1962). Neumann (1963) later proposed a simple control system where chamber pressure is manipulated in order to maintain the product at the desired temperature; this was obtained either by means of a throttling valve connecting the chamber to the

condenser, or acting on the condenser temperature. Willemer (1987) showed an example of nominal-actual value regulation of the shelf temperature, measurement of the product temperature by BTM and its control by manipulation of the chamber pressure during the sublimation phase. The thermodynamic lyophilization control system was later described by Oetjen (1999) and by Oetjen and Haseley (2004): it uses the results of the BTM algorithm and a set of heuristics for the calculation of the control actions.

Tang *et al.* (2005) and Pikal *et al.* (2005) proposed, and patented, an expert system, named SMART™ Freeze-Dryer, for manipulating the shelf temperature and the chamber pressure using a simple model and the results obtained by means of the MTM algorithm. Gieseler *et al.* (2007b) validated experimentally the SMART Freeze-Dryer with different types of excipients, formulations (involving crystalline and amorphous products) and vials, evidencing that the algorithm can be a useful tool for development of a lyophilization cycle during a single freeze-drying run, but the quality of the cycle optimization is dependent upon the accuracy of the parameters which must be provided by the user (e.g., collapse temperature, vial cross-sectional area).

Tenedini and Bart (2001) patented a method for monitoring both the primary and the secondary drying by using the measurements provided by a windmill sensor and some "rules of thumb". Moreover, they proposed to save energy by automatically disabling the vacuum pump when the pressure in the process chamber falls below a predefined set-point; the vacuum source is then reconnected if the process chamber pressure rises above a second predefined set-point. They pointed out that by controlling pressure within the process chamber only through selective connecting/disconnecting of the vacuum pump, a higher level of product purity is achieved compared with the conventional requirement of an inert gas bleed system, while still providing a comparable level of pressure control. The speed of freeze-drying can also increase as a consequence of the higher specific heat of the water vapor (that is the prevalent species in the chamber) with respect to the inert gas.

In a patent by Lambert and Wang (2003) it is proposed to monitor in-line the cake resistance by inserting a tube in some vials and measuring the pressure drop of an inert gas; it is suggested that the results from the measuring system are used to provide a control signal to a control system, but it seems difficult to really apply the proposed method, even in a laboratory apparatus.

Barresi *et al.* (2009a, c) proposed to use DPE in a control loop where the heating fluid temperature is manipulated. This control algorithm, named *LyoDriver*, uses the estimations obtained by means of the DPE algorithm (product temperature, heat transfer coefficient between the heating fluid and the product at the bottom of the vial, and the diffusivity coefficient of the vapor in the dried layer), as well as some process variables (i.e., the temperature of the fluid, the pressure in the chamber, and the cooling rate of the freeze-dryer) and a simplified mathematical model for the primary drying (Velardi and Barresi, 2008a). In order to run *LyoDriver* the user must set the values of the prediction horizon (h_p), i.e. the number of time for which the controller computes a proper heating policy on the basis of the prediction of evolution of product temperature, and the time between a control action and the next one.

After that, *LyoDriver* calculates a sequence of suitable set-points for the fluid temperature ($T_{\text{fluid,sp}}$), one for each control interval all through the prediction horizon, in such a way that the product temperature is as close as possible to its target. At the beginning of primary drying, when the temperature of the product is well below the upper limit, the heating fluid temperature is raised at its maximum rate compatible with the actual machine capacity and, in this way, the product approaches its limit as fast as possible. After this first step, a PRT is performed and *LyoDriver*, using the DPE algorithm, estimates the time-varying product temperature at the bottom of the vial (where the temperature is higher) over the whole prediction horizon and recalculates the optimal heating policy accordingly to the current system state. This is regularly repeated at each successive DPE run so that potential mismatches between the *LyoDriver* model predictions and the actual process behavior can be taken into account. If the estimated product temperature approaches its limit, *LyoDriver* reduces the shelf temperature in such a way that the product is maintained below its target. Another point to be stressed is that the shelf temperature evolution is calculated taking into account the real dynamics of the heating and cooling systems.

Two control algorithms have been proposed and compared: the former is a simple feedback controller that calculates the control action as a function of the difference between the product temperature at the bottom of the vial and the maximum allowed value, while the latter relies on a model-based algorithm that calculates the fluid temperature to maintain the temperature of the product at the bottom of the vial equal to the maximum value (Pisano *et al.*, 2010a). Both control laws use an unsteady-state model of the process, made of a set of equations that supplies the evolution of both product temperature and frozen layer thickness. These equations are integrated from the initial time (t_0), which is zero for the first run and equal to the time elapsed from the first test in next ones, up to the prediction horizon (t_N) set by the user, or up to the estimated end-point of the primary drying phase, that corresponds with the time at which the frozen layer thickness is equal to zero (t_{N^*}). If the feedback logic with a simple proportional controller is used, the optimal heating strategy is calculated throughout all the prediction horizon considering the optimal sequence of set-point shelf temperatures as a piecewise-linear function, according to the relationships:

$$\begin{aligned}
&t_0 \le t < t_1 \quad \Rightarrow \quad T_{\text{shelf,sp}} = T_{\text{shelf}}(t_0) + K_{\text{P}}(T_{\text{B}}(t_0) - T_{\text{B,sp}}) \\
&t_1 \le t < t_2 \quad \Rightarrow \quad T_{\text{shelf,sp}} = T_{\text{shelf}}(t_1) + K_{\text{P}}(T_{\text{B}}(t_1) - T_{\text{B,sp}}) \\
&\vdots \\
&t_{N-1} \le t < t_N \quad \Rightarrow \quad T_{\text{shelf,sp}} = T_{\text{shelf}}(t_{N-1}) + K_{\text{P}}(T_{\text{B}}(t_{N-1}) - T_{\text{B,sp}})
\end{aligned} \tag{4.16}$$

Here, $t_j - t_{j-1}$ defines the time interval between two control actions, K_{P} is the proportional gain of the controller, $T_{\boldsymbol{B}}(t_j) - T_{\text{B,sp}}$ is the difference between the product temperature at the bottom of the vial and its set-point, that is the temperature to which the product has to be driven. One aspect to be stressed is that the set-point of T_{B} might be lower than the target temperature set by the user, because the controller iteratively calculates a new target in order to guarantee that possible temperature overshoots in

the prediction horizon are maintained under the maximum temperature allowed by the product. Moreover, *LyoDriver* calculates $T_{B,sp}$ also taking into account temperature rises caused by regular PRTs. The control interval usually corresponds to the time between two subsequent PRTs and only the first control action of the calculated sequence is actually applied: the heating policy is regularly recalculated after the system state has been updated. As an alternative, more control actions can be applied between a DPE and the next one in order to disturb less the dynamics of the process. The value of the gain of the controller has to be calculated using some performance criteria, for example, the minimization of the integral square error (ISE) between the product temperature and the set-point value from the current time (t_0) up to the prediction horizon (t_N):

$$\min_{K_P}(ISE) = \min_{K_P} \int_{t_0}^{t_N} (T_{B,\text{predicted}}(t) - T_{B,sp})^2 \mathrm{d}t \tag{4.17}$$

The simplified model of Velardi and Barresi (2008a) is used to estimate the time evolution of the product temperature required by Eq. 4.17.

If a model-based approach is implemented, the optimal sequence of shelf temperature set-points throughout the prediction horizon is calculated as a piecewise-linear function in such a way that the bottom product temperature is equal to the target value. Again, the simplified mathematical model of Velardi and Barresi (2008a) can be used for this purpose:

$$\begin{aligned}
&t_0 \le t < t_1 \quad \Rightarrow T_{\text{shelf},sp}(t) = T_{B,sp} + (T_{B,sp} - T_i(t_0)) \left[K_v \left(\frac{1}{K_v} + \frac{L_{\text{frozen}}(t_0)}{\lambda_{\text{frozen}}} \right) - 1 \right]^{-1} \\
&t_1 \le t < t_2 \quad \Rightarrow T_{\text{shelf},sp}(t) = T_{B,sp} + (T_{B,sp} - T_i(t_1)) \left[K_v \left(\frac{1}{K_v} + \frac{L_{\text{frozen}}(t_1)}{\lambda_{\text{frozen}}} \right) - 1 \right]^{-1} \\
&\vdots \\
&t_{N-1} \le t < t_N \Rightarrow T_{\text{shelf},sp}(t) = T_{B,sp} + (T_{B,sp} - T_i(t_{N-1})) \left[K_v \left(\frac{1}{K_v} + \frac{L_{\text{frozen}}(t_{N-1})}{\lambda_{\text{frozen}}} \right) - 1 \right]^{-1}
\end{aligned} \tag{4.18}$$

The considerations about the target temperature ($T_{B,sp}$) and the control interval made for the feedback algorithm can be extended to the model-based controller.

Both control algorithms take into account the actual thermal dynamics of the freeze-dryer, that is, the actual cooling and heating rates:

$$T_{\text{shelf}}(t) : \begin{cases} \dfrac{\mathrm{d}T_{\text{shelf}}}{\mathrm{d}t} = r & t_{j-1} \le t < t_{sp,j} \\ T_{\text{shelf}}(t) = T_{sp,j} & t_{sp,j} \le t < t_j \end{cases} \tag{4.19}$$

where $t_{sp,j}$ is the time when the set-point is reached and the temperature T_{shelf} is not changed anymore, given by:

$$t_{sp,\,j} = t_{j-1} + \int_{T_{shelf}(t_{j-1})}^{T_{shelf,sp,j}} \frac{1}{r}\,dT_{shelf} \tag{4.20}$$

The process dynamics is thus simulated over h_p using the simplified model of Velardi and Barresi (2008a) and taking into account that the shelf temperature changes according to the actual cooling and heating rates and is kept constant once the set-point has been reached.

The drying time, resulting when the model-based controller is used, is slightly higher than that obtained through the feedback algorithm, but the simpler mathematical formulation, since no optimization is involved in the calculation, and the smaller computation time make the model-based approach more suitable for in-line control (Pisano *et al.*, 2010a).

Figure 4.17 shows two examples of the results that can be obtained when *LyoDriver* is used to manage the process: the ice temperature at the bottom of the vial estimated by DPE is shown, as well as the value of the temperature of the heating fluid in the case of the feedback controller (Fig. 4.17a) and of the model-based controller (Fig. 4.17b). It can be observed that the estimated maximum product temperature never went over the limit value fixed by the user and, thus, the maximum allowable heating rate is obtained throughout all primary drying, minimizing the duration of this step. The product temperature rise during a PRT is taken into account when the heating policy is calculated: as a consequence, the value of the product temperature estimated by DPE is slightly lower than the maximum value given by the user and, as is shown by the temperature measurement given by a thermocouple placed in the bottom of a vial, the product temperature never went over its limit, not even during the PRT.

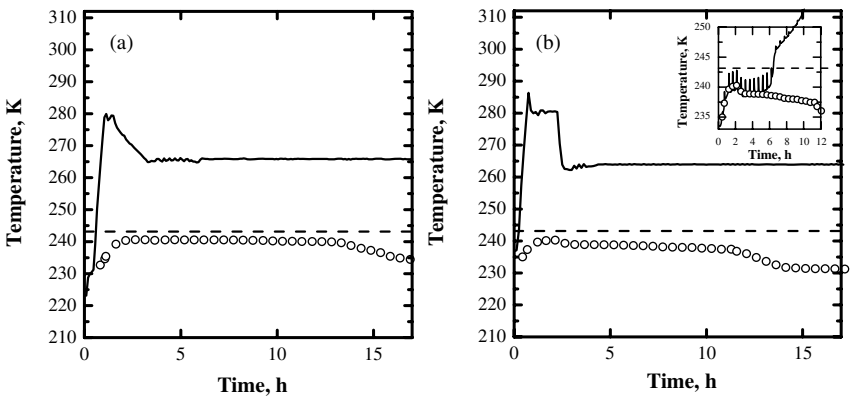

Fig. 4.17 Examples of the application of *LyoDriver* to control a freeze drying process of 10% solution of sucrose ($d_v = 14.2 \times 10^{-3}$ m, $L_p = 7.2 \times 10^{-3}$ m, $P_c = 10$ Pa). Results obtained using the feedback controller are shown in (a) ($N_v = 175$), while results obtained using the model-based controller are shown in (b) ($N_v = 205$). The time evolution of the shelf temperature (solid line), of the maximum product temperature estimated by DPE (symbols) and the limit temperature (−30 °C, dashed line) are shown; the product temperature measured by a thermocouple is shown in the insert in (b).

It can be noted that when the primary drying is approaching the end, the product temperature estimated by means of the DPE algorithm decreases: this is typical behavior for all MTM type approaches (Tang *et al.*, 2005; Oetjen and Haseley, 2004) and DPE also has this defect, mainly caused by heterogeneity of the batch, as discussed in the previous section. This behavior must be taken into account when setting the parameters of the control algorithm and in the last part of the cycle it is advisable to use the sequence of control action suggested in the previous step, without updating based on the new (misleading) measurements. The same problem was evidenced also by Gieseler *et al.* (2007b) when using the SMART™ Freeze-Dryer, and by Willemer (1991), using a BTM-based control system. The last author evidenced that the role of the control system is important in the first part of the cycle, suggesting to disconnect it in the second part of the cycle. This is correct, except when the process becomes mass transfer controlled: in this case the action of the control system is fundamental.

The use of a model predictive control (MPC) algorithm has been recently proposed by Daraoui *et al.* (2008): a detailed mathematical model is used (Sadikoglu and Liapis, 1997) in an algorithm that combines the internal model control (IMC) structure and the MPC framework to correct the modeling errors introduced in the model-based optimization. The manipulated variable is the shelf temperature and the goal is the minimization of the drying time; constraints on the manipulated and on the controlled variables can be easily taken into account in the optimization algorithm.

In both examples of Fig. 4.17, the heat transfer from the shelf controlled the sublimation rate and the fluid temperature was usually maintained almost constant in the second part of the drying. Here, the value of the shelf temperature ensured the maximum sublimation rate, since it was significantly greater than the product temperature and the chamber pressure was not very influential. In some cases the fluid temperature calculated by the controller can approach the product temperature, thus indicating that the vapor transport through the solid matrix controls the drying rate: the proposed control system is still effective since it guarantees product integrity and the maximum flow rate at that pressure, but an in-line change in the chamber pressure might reduce the drying time (Fissore *et al.*, 2009a).

As discussed before, the continuous manipulation of the chamber pressure can be very effective because it guarantees rapid response and because it affects the sublimation rate, both when the system is mass transfer controlled, modifying the driving force, and when heat transfer is limiting, modifying the heat transfer coefficient, that significantly depends on pressure. The possibility of manipulating simultaneously the temperature of the shelf and the pressure in the drying chamber has been recently investigated by Pisano (2009): a MPC algorithm has been proposed and demonstrated to be able to guarantee product quality and to minimize the time required to complete the main drying (Pisano *et al.*, 2010b).

As pointed out in the previous section, the batch of vials can exhibit a significant degree of heterogeneity due to radiation, water vapor hydrodynamics, inert distribution and non-uniform shelf temperature. Thus, a control logic based on the estimation of the mean state of the whole batch could be inadequate in certain

situations: as an alternative, the control action can be calculated on the basis of the actual status of a single vial, for example, the vial whose temperature is supposed to be higher, using an observer as sensing device. Fissore *et al.* (2008a) proposed a simple control loop based on a feedback logic where T_{shelf} is manipulated in order to maintain the product temperature, estimated by a soft-sensor, at the maximum allowed value. The control law can be a conventional proportional-integral (PI) compensator:

$$T_{shelf}(t) = -K_P\varepsilon(t) - K_I\int_{t_0}^{t}\varepsilon(t)dt + T_{shelf,0} \tag{4.21}$$

$$\varepsilon(t) = \hat{T}_{p,max}(t) - T^*_{p,max} \tag{4.22}$$

The control action is taken when the maximum temperature of the product estimated by the observer, $\hat{T}_{p,max}$, approaches the limit value $T^*_{p,max}$, $\varepsilon(t)$ is the difference between the actual value of $\hat{T}_{p,max}$ at time t and the target value $T^*_{p,max}$, t_0 is the starting time of the control action, when the value of the manipulated variable is $T_{shelf,0}$. The proportional mode adjusts the controller signal in proportion to the error, according to the parameter K_P; the integral mode is required to eliminate the offset between the set-point and the process value, according to the parameter K_I. The values of the parameters of the PI controller are calculated in order to minimize the ISE:

$$\min_{K_P,K_I}(ISE) = \min_{K_P,K_I}\int_{t_0}^{t}(T_{p,max,predicted}(t) - T^*_{p,max})^2 dt \tag{4.23}$$

where $T_{p,max,predicted}$ is the maximum product temperature predicted by the detailed model of the process, which is integrated over time, starting from the knowledge of the process parameters provided by the observer at time t_0. In this way, the tuning of the compensator is performed with an adaptive strategy in which the controller parameters are iterated until a minimum of the ISE is reached, and the obtained values of K_P and K_I are finally implemented in the control law expressed by Eqs. 4.21 and 4.22. Figure 4.18 shows the results obtained when simulating a process with this feedback controller and with a Kalman filter observer that uses the measurement of the external temperature at the bottom of the vial (Barresi *et al.*, 2009b, c). The target value of the product temperature is 245 K; the shelf temperature is initially ramped up to $T_{shelf} = 273.15$ K: after about 4 h from the beginning of the operation the observer predicts that the limit temperature has been reached and the control action is taken, thus regulating the value of T_{shelf} according to Eq. 4.21.

If the batch is highly heterogeneous various observers can be used to track the dynamics in several vials placed at different positions in the drying chamber and the highest product temperature can be used by the controller to manipulate the shelf temperature.

As an alternative, the hybrid monitoring system obtained by coupling the DPE and the "smart vial" observer previously described can be used in the control loop: preliminary results have demonstrated the feasibility of such an approach (Barresi *et al.*, 2009c).

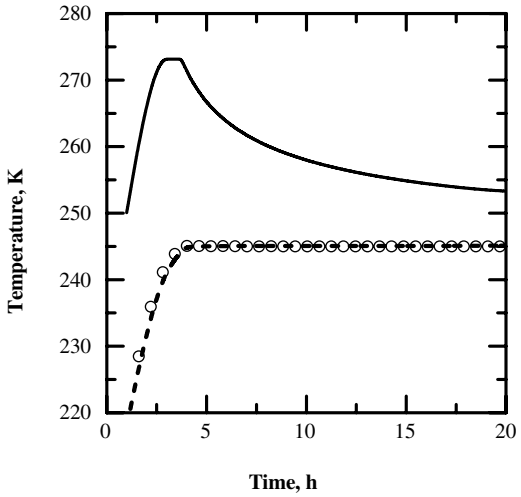

Fig. 4.18 Example of the application of the feedback control strategy that uses the observer to estimate the maximum product temperature (the freeze-dried product is skimmed milk; $d_v = 14.2 \times 10^{-3}$ m, $L_p = 8 \times 10^{-3}$ m, $P_c = 5$ Pa): time evolution of the shelf temperature (solid line), of the maximum product temperature estimated by the observer (dashed line) and of the true maximum product temperature (symbols) during the primary drying phase.

4.5
Monitoring and Control of Secondary Drying

Secondary drying has to be carefully monitored in order to know when the desired amount of residual solvent content in the product is achieved. Tang and Pikal (2004) proposed to monitor this stage by extracting samples from the freeze-dryer without interrupting the process (using a "sample thief") and measuring their solvent content by means of Karl Fischer titration, thermal gravimetric analysis, or near infra-red spectroscopy: when the residual solvent content has reached the target value, secondary drying can be considered complete. As an alternative, the endpoint of secondary drying can be detected qualitatively by using a cold plasma ionization device (Mayeresse *et al.*, 2007) as discussed in Section 4.3; the same device has also been demonstrated to be useful in monitoring qualitatively the kinetics of water desorption.

Other methods proposed in the past to monitor secondary drying are based on the estimation of the solvent flow rate that can be obtained, for example, from the PRT. This technique can be tracked back to the early 1960s, as was proposed by Kan (1962) for detection of the drying endpoint. In fact, the mass flow rate of water (or solvent) $\dot{M}_w$ can be calculated from the slope of the curve of chamber pressure vs. time at the beginning of the PRT:

$$\dot{M}_{\mathrm{w}} = \tilde{M}_{\mathrm{w}} \frac{V_{\mathrm{c}}}{\tilde{R} T_{\mathrm{c}}} \frac{\mathrm{d}P_{\mathrm{c}}}{\mathrm{d}t}\Big|_{t=t_0} \tag{4.24}$$

The loss of water (or solvent) during the time interval elapsed between two consecutive PRTs can be estimated assuming a constant value of the flow rate $\dot{M}_{\mathrm{w}}$ in that interval that is:

$$\Delta w_k = \dot{M}_{\mathrm{w},k} \Delta t_k \tag{4.25}$$

where Δt_k is the time elapsed between the $(k-1)$th PRT and the kth PRT, Δw_k is the loss of water during the time interval Δt_{k} and $\dot{M}_{\mathrm{w},k}$ is the mass flow of water (or solvent) from the product calculated from the kth PRT. The total amount of water (or solvent) removed between a reference time t_0 (e.g., the start of the secondary drying) and any given time of interest t_i is simply the summation of all the Δw_k occurring in the intervals between the various PRTs from t_0 to t_i. Moreover, if one value of residual water content at a reference time, for example, at the end of primary drying, is available, the actual moisture content vs. time can be calculated (Oetjen and Schilder, 2003; Tang *et al.*, 2005; Pikal *et al.*, 2005).

Willemer (1991) proposed to relate the pressure increase as a consequence of the PRT during secondary drying to the residual moisture content using this measure to stop secondary drying. An improved approach is that proposed by Oetjen (2001): using two successive measurements of desorption rate, calculated from the water flow rate $\dot{M}_{\mathrm{w}}$:

$$r_{\mathrm{d,exp}} = \frac{\dot{M}_{\mathrm{w}}}{m_{\mathrm{dried}}} \tag{4.26}$$

it is possible to extrapolate the point in time at which the desorption rate will reach a given small value. This method is shown to fail when secondary drying is finishing.

Fissore *et al.* (2008b, 2011b) proposed an innovative approach to determine the residual water content of the dried product vs. time and to give a reliable estimation of the time that is necessary to complete secondary drying, that is, to fulfill the requirement on the final water content of the product. The method uses the values of water (or solvent) desorption rate that can be calculated from the PRT (Eq. 4.26) and a mathematical model that describes the change with time of the residual water content in the dried product. To this purpose it is required to model the dependence of the desorption rate of water (or solvent) from the residual water content in the product. Various models have been proposed in the literature: the desorption rate can be assumed to be proportional to the residual water content, or to the difference between the residual water content and the equilibrium value. It is possible to use the exact mechanism, if it is known. Otherwise the first-mentioned model, that is much simpler and that has been demonstrated to describe adequately the process (Liapis and Bruttini, 1995) can be applied:

$$r_{\mathrm{d}} = -k_{\mathrm{d}} X \tag{4.27}$$

The time evolution of the residual moisture content X, in kg of water per kg of dried mass, is given by the integration of the following differential equation:

$$\frac{dX}{dt} = r_d = -k_d X \tag{4.28}$$

k_d is the kinetic constant of the process: it can be a function of the temperature and, thus, it can change with time as the temperature of the product can change with time, in particular at the beginning of the secondary drying when the temperature has risen from the value used during primary drying to that of the secondary drying. If one PRT is made at $t = t_{k-1}$ and the successive test is made at $t = t_k$ and the product temperature, that is slightly varying in that interval, is assumed to be constant, the variation in the moisture content in the solid can be described by:

$$\frac{dX}{dt} = r_{d,k-1} = -k_{d,k-1} X \tag{4.29}$$

Solution of Eq. 4.29 requires the initial condition, that is, the value of the residual moisture content X at $t = t_{k-1}$; this value can be calculated from the time integration of Eq. 4.29 in the previous time interval. This procedure can be iterated until the value of the residual moisture content $X_0 = X(t_0)$ at the beginning of the secondary drying stage ($t = t_0$) appears; thus, in the time interval between t_k and t_{k-1} the evolution of the residual moisture content is given by:

$$X = X_0 \prod_{r=1}^{k-1} e^{-k_{d,k-1}(t_r - t_{r-1})} e^{-k_{d,k-1}(t - t_{k-1})} \tag{4.30}$$

and the theoretical value of the desorption rate in this time interval is:

$$r_{d,\text{theor},k} = -k_{d,k} X_0 \prod_{r=1}^{k-1} e^{-k_{d,k-1}(t_r - t_{r-1})} e^{-k_{d,k-1}(t - t_{k-1})} \tag{4.31}$$

The experimental values of the desorption rates obtained until t_k are compared with the theoretical values that depend on the kinetic constants and on X_0: these parameters can thus be identified by optimizing the fit between model predictions and experimental values. Finally, it is possible to estimate the time required to complete secondary drying, that is, to achieve the target value of X (or of r_d), by introducing the target value in the left-hand side of Eq. 4.30 (or of Eq. 4.31) and solving for the time t. After each PRT a new value of the desorption rate is available and a better estimation of X_0, of the kinetic constant and, thus, of the time required to complete secondary drying, is obtained. In the proposed approach it is no longer required to know the value of the initial water content, as this value is estimated by the algorithm; similarly, it is no longer necessary to extract any samples from the drying chamber and to use expensive sensors. A series of experiments were carried out to validate this method. Figure 4.19 shows an example of the results that can be obtained: the experimental values of the desorption rate have been obtained by means of the PRT, while the estimations of the residual water content are compared with the values obtained by weighing some vials taken from the drying chamber using a sample thief. When secondary drying is started the shelf temperature is increased and, during this time interval, the product temperature, and thus the desorption rate, increases; then, the temperature remains constant and, due to the lowering of the residual water content, the desorption rate decreases.

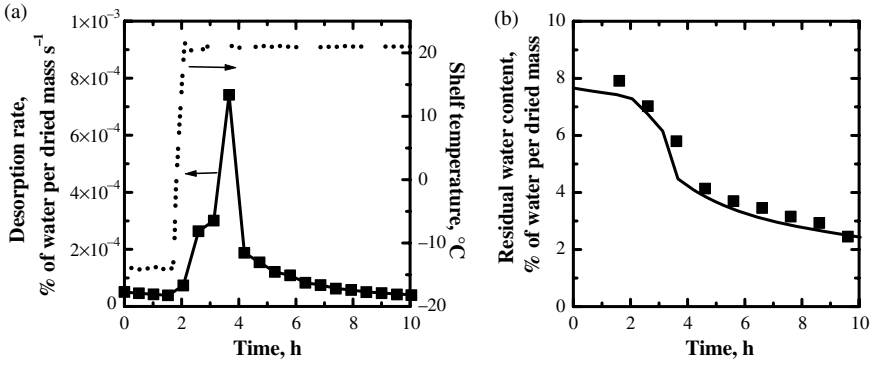

Fig. 4.19 Comparison between experimental values (symbols) and values predicted by the proposed algorithm (solid lines) for the desorption rate (a) and for the residual water content (b). The time evolution of the shelf temperature is also shown (dotted line). Data refer to a freeze-drying cycle of 20% by weight aqueous solution of sucrose ($N_v = 155$, $d_v = 20.85 \times 10^{-3}$ m, $L_p = 9.8 \times 10^{-3}$ m): freezing was carried out at −50 °C for 17 h, primary drying was carried out at −15 °C and 10 Pa for 25 h. Time is set equal to zero at the beginning of the secondary drying.

It is worth noticing that secondary drying is carried out at a higher temperature than primary drying due to the lower value of the residual water content and, thus, the higher glass transition temperature. At a given temperature the water content decreases with time until it becomes rate limited: raising the temperature increases the rate of water removal until a new rate-limiting plateau is reached. The plateau effect demonstrates that products cannot be adequately dried to low water contents by carrying out secondary drying at low temperatures, unless very extended and uneconomical drying periods are used. As water is removed, the glass transition temperature rises and the product temperature may then be increased; more water diffuses out, thus raising again the glass temperature, and the product temperature may be further increased (Franks, 2007). Increasing the product temperature is thus necessary, but if the temperature of the product is raised at a rate such that it increases faster than the increase in the glass transition temperature resulting from water removal, then collapse can occur. A few papers have appeared in the literature about the control of the secondary drying step. Sadikoglu *et al.* (1998) proposed to manipulate the heating and the total pressure in the drying chamber in order to minimize the time required to get the desired amount of residual water in the product; a constraint is placed on the maximum product temperature. Variational calculus, involving a detailed multidimensional model of the process, was used by Sadikoglu (2005) to optimize the secondary drying. Pikal *et al.* (2005) proposed to adjust the shelf temperature in order to reach the desired level of water in the product: they formulate some heuristics to select the shelf temperature and the heating rates for crystalline products, crystalline bulking agents and non-crystalline formulations. A model-based control algorithm was proposed by Trelea *et al.* (2007) to maximize process productivity besides ensuring product quality preservation, taking into account the variation of the glass transition temperature with the residual water content.

4.6
Quality by Design

As highlighted in the previous sections about monitoring and control of a vial freeze-drying process, one of the most important issues that has to be taken into account for product quality monitoring is batch heterogeneity: during the process both product temperature and residual water content in the various vials are not uniform, there exists a wide (or narrow) distribution around a mean value for both variables.

In Section 4.3 we have shown how it is possible to take into account this issue when monitoring the whole batch (e.g., by use of the parameter γ in the DPE algorithm, which is a very simple approach and, thus, it requires further improvement), while in Section 4.4 we have described a control system that uses a soft-sensor to monitor selected vials placed in different positions in the drying chamber and manipulates the shelf temperature on the basis of the highest product temperature: the control policy is thus much more conservative and this increases the duration of the process. Hence, it should be clear by now that batch heterogeneity poses serious problems to the monitoring system and requires the use of a much more conservative control algorithm to guarantee product quality. It is, therefore, worth investigating the various causes of batch heterogeneity, providing guidelines for an optimal design of the equipment and of the process that can result in a more uniform batch. This is in agreement with the spirit of the previously cited Guidance for Industry PAT that encourages an understanding of the manufacturing process, that is, to identify and explain all critical sources of variability, and, finally, to manage variability in the process. The main sources of variability in a vial freeze-drying process are the following (compare also with Chapter 3, Section 3.2.4):

- **Shelf Temperature**: A maximum temperature difference of about 2 K between two points of each shelf currently occurs in well-designed industrial scale equipment, while a difference up to 3 K is often observed in small scale units used for recipe development and research purposes.
- **Radiation from Chamber Walls and from the Door**: This is a well known source of inter-vial variance (Gan *et al.*, 2004, 2005a, b). Kobayashi *et al.* (1991) and Oetjen and Haseley (2004) investigated the possibility of acting on the wall temperature in order to achieve higher uniformity in the batch, and a system that controls the temperature of the chamber walls has also been patented (Sennhenn *et al.*, 2005).
- **Fluid Dynamics in the Drying Chamber**: In the past, the role played by water vapor fluid dynamics was assumed to be negligible, also because of the difficulty to identify and isolate its effects from the experimental results. Nowadays computational fluid dynamics (CFD) offers the possibility to investigate complex industrial processes; for example, Rasetto *et al.* (2008) and Rasetto (2009) studied the effect of some geometrical parameters of a drying chamber (clearances between the shelves and position of the duct leading the vapor to the condenser) on the fluid dynamics of the water vapor as a function of the sublimation rate, both in a small scale (chamber volume of about 0.2 m^3) and in an industrial scale

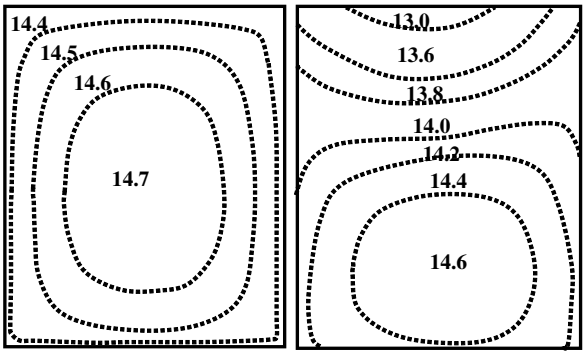

Fig. 4.20 Contour plot of the absolute pressure (Pa) on (a) the 1st tray and on (b) the 12th tray in a freeze-drying chamber with 16 trays when the sublimation flow rate is 0.7 kg h^{-1} m^{-2} (the trays are numbered from the bottom to the top of the chamber). Operating conditions: $T_{shelf} = 258$ K, $T_i = 239$ K, reference pressure = 10 Pa, dimensions of a shelf = 1500 mm × 1800 mm, distance between the shelves = 93.5 mm.

apparatus (chamber volume of about 10 m^3). Their results evidenced the presence of significant pressure gradients along the shelves, in particular in the large scale unit (Barresi *et al.*, 2008a, 2010). Figure 4.20 shows an example of the pressure distribution in a large-scale unit. Apart from geometrical characteristics of the drying chamber, also the value of the sublimation rate affects the difference between the total local pressure and the value at the border of the shelf (ΔP) as it is possible to see in Fig. 4.21.

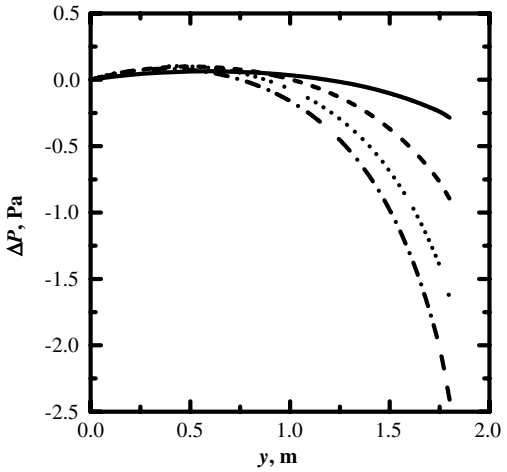

Fig. 4.21 Pressure drop along the centerline of the 12th shelf for various values of mass flux (_____: 1, _ _ _ _: 0.7, ...: 0.35, and _._._._: 0.15 kg h^{-1} m^{-2}); reference pressure = 10 Pa, $T_{shelf} = 258$ K, $T_i = 239$ K, total chamber volume = about 10 m^3, number of shelves = 15, dimensions of a shelf = 1500 mm × 1800 mm, distance between the shelves = 93.5 mm.

A two-scale model coupling the detailed simulation of the dynamics in each vial with the results obtained using CFD to model the fluid dynamics in the chamber can be useful to simulate the dynamics in single vials placed in particular positions (e.g., where the radiation effects are more important or where the pressure is higher), as well as that of the whole batch, thus calculating the mean value of the product temperature and of the residual water content, as well as the standard deviation around this mean value. A simplified model describing the evolution of each single vial can be directly implemented in the CFD code, for example, by means of user-defined functions, even if this increases the time required for the simulations, besides posing convergence problems; moreover, only simple models can be implemented in a CFD code and, therefore, this approach is preferable only when a certain degree of uncertainty in the results about the time evolution of the product is acceptable (Rasetto, 2009). When the time evolution of the product has to be estimated with the best possible accuracy, other approaches must be used, involving a detailed one-dimensional model for the vials (e.g., the model of Velardi and Barresi, 2008a). A simple and efficient iterative algorithm that couples the detailed simulation of the dynamics in each vial with the results obtained using CFD to model the fluid dynamics in the chamber has been proposed (Barresi *et al.*, 2008b; Rasetto *et al.*, 2010):

1) At a generic time t, given the values of T_{shelf} (known from the measured, or modeled, distribution of shelf temperature) and of P_c (known from CFD calculations), the sublimation flux (and the residual water content and the product temperature) at time $t + \Delta t$ are calculated by integrating the detailed one-dimensional model. This assumes that T_{shelf} and P_c do not vary significantly in the time interval Δt, that is, that the variation of the sublimation flow rate is small: this assumption is reasonable if a small time interval Δt is used, for example, 30 min.
2) At time $t + \Delta t$, the new value of P_c is calculated using the CFD model (either carrying out new CFD simulations, or using correlations obtained from a previous CFD campaign of simulations) and the previously calculated sublimation flux as boundary condition.
3) Steps 1 and 2 are repeated until the end of primary drying is reached.

Figure 4.22 shows an example of the results that can be obtained: the time evolution of the mean value of the interface temperature on the 1st (at the bottom of the drying chamber) and on the 12th shelf in a large-scale equipment is shown. On the 1st tray the standard deviation of the interface temperature of the vials is very low (because of the low pressure gradients) and thus the mean value is representative of the behavior of the vials placed on that shelf, while higher values of the standard deviation are observed on the 12th tray: in this case the interface temperature is not uniform and the dynamics exhibited by the various vials can be significantly different.

Similar calculations can be done for the vials of the other shelves of the batch, thus giving the mean value and the standard deviation of the interface temperature and position in the whole chamber: both values could be used for monitoring and control purposes and the spread in the distribution of the value of interest should be taken into account by manufacturers in the design of equipment and in choosing the operating conditions. Moreover, the two-scale model allows quantitative evaluation of

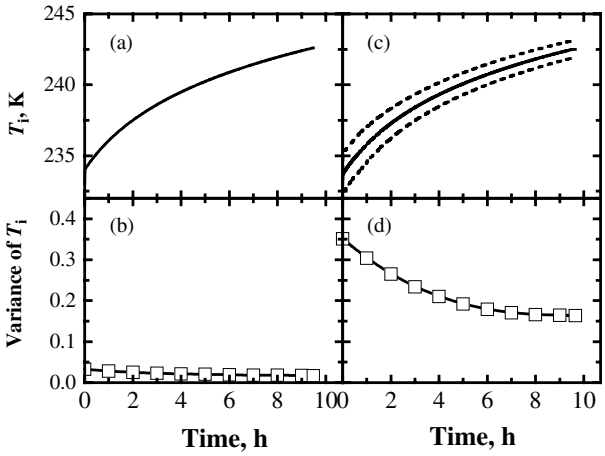

Fig. 4.22 Time evolution of the mean value of the interface temperature ((a) and (c), solid lines) and of the standard deviation ((b) and (d)) for the vials on the 1st ((a) and (b)) and on the 12th ((c) and (d)) shelves during the freeze-drying of a 5% solution of Bovine Serum Albumin in vials having a total volume of 4 ml ($L_{frozen} = 7.2 \times 10^{-3}$ m, $T_{shelf} = -15\,^{\circ}C$, operating pressure = 10 Pa, distance between the shelves = 93.5 mm). Dashed lines identify the upper and lower bounds of the interface temperatures in the vials.

the influence of the size of the apparatus, of the geometric characteristics of the chamber, and of the operating parameters and, thus, it can be very useful in process scale-up and process transfer. Finally, it can be employed as a design tool, to improve the performance of the drying chamber and to improve the performance and the accuracy of the sensors in the drying chamber, taking into account actual gradients and delay times (Rasetto *et al.*, 2009).

4.7 Continuous Freeze-Drying

Significant improvements with respect to process monitoring and control could be obtained if freeze-drying was carried out using a continuous process. Semi-continuous and continuous equipment have been designed and built for the food industry in the last decades: the main advantage is that such processes are easy to control and give manufactured products a standard uniform quality. The possibility of also using continuous equipment for freeze-drying of pharmaceuticals has been proposed and prototypes have been designed. Jennings (1999) described a process for continuous freeze-drying in vials and carried out a comparison with the corresponding batch operation, evidencing that continuous operation makes it possible to reduce significantly the drying time, thus making the process competitive. Rey and May (2004) suggested a different technical solution: they proposed that the initial solution is distributed as individual droplets frozen into spherical granules of given geometry, continuously fed into a vacuum chamber, and spread on a heated conveyor. On that

tray they glide self-suspended on their water vapor cushion as a thin, regular, fluidized cloud at a well controlled operating pressure fit for sublimation. At the end of the tray they reach a transfer lock which discharges them onto another conveyor placed in a second chamber, fit for desorption and secondary drying. Finally, they enter an ultimate lock and are discharged into a receiving bin under a dry neutral atmosphere. The efficiency of such a process could be tremendous, with very short drying times in the case of small size granules. At the end of the process, the result is a population of granules, all dried under the same conditions, all equal in quality and size, that can be numbered and fed into dry sterile vials. There are still a number of technical issues that have to be solved, but industrial solutions to those specific problems exist: it is necessary to change mindset, to accept a new approach that deviates from historical practice, and this can be much more difficult to achieve.

4.8 Conclusion

Since during the primary drying product damage can occur, monitoring and controlling this phase is very important to guarantee the desired final product quality; in particular, product temperature has to be maintained below the collapse (or melting) value during the cycle.

Besides the temperature, the residual amount of water also has to be monitored in order to detect the endpoint of the primary drying. Secondary drying has to be started only when primary drying is completed: if secondary drying is started before, the product temperature may exceed the maximum allowed value, while if secondary drying is delayed, the cycle is not optimized and the cost of the operation increases. Finally, the residual water content at the end of secondary drying has to be monitored: for most products the target level of residual water is very low, even if for certain products it has been demonstrated that a too low level of residual water should be avoided.

The attainment of the goal is made more difficult by the fact that the vials do not undergo the same freeze-drying history; the most critical step to be controlled is freezing, because the structure generated in this step will strongly influence the following stages, but this is, at the moment, the more difficult step to control in industrial production. Also, the conditions during drying are responsible for variance, not only because of the well known radiation effect, or because the shelf temperature is not uniform, but also because of the flow field inside the freeze-dryer chamber. Moreover, while in small-scale units, used for recipe development, radiation from chamber walls plays an important role, in the industrial-scale apparatus the role of pressure gradients is much more important: this has to be taken into account during process scale-up.

It is thus clear that in order to manage a freeze-drying process we need an efficient monitoring and control system, as has been recently pointed out by the Guidance for Industry PAT (Process Analytical Technology) issued by the US Food and Drug Administration in 2004. To this purpose the development of model-based monitoring tools is encouraged.

In this chapter the current state of the art as concerns monitoring of the process has been critically reviewed, pointing out that in order to be applicable in predictive control systems, measuring devices should be able to supply the full state of the system, that is, not only the product temperature but also the residual ice or moisture content, and some physical characteristics or process parameters, such as the cake resistance to flow, and the shelf to product heat transfer coefficient.

Different off-line and in-line control strategies have been discussed: a new approach to the process control has been considered, presenting possible solutions based either on the average batch monitoring (in vials or in bulk), or on single vial monitoring; in particular, a model-based control tool, *LyoDriver*, has been presented and shown to be effective in controlling and optimizing a freeze-drying cycle in both pilot-scale and industrial apparatus. It is important to highlight that the use of an active control system, that can react to eventual disturbances, changes of input conditions, and lot variability, can allow one to avoid product failure: as an example, it can take into account changes in the heating and cooling rate of the apparatus, can guarantee safe operation even when the process becomes mass-transfer controlled, and can find the optimal conditions, without impairing the product quality, when the pressure in the chamber is varied, either as a consequence of a change in set-point, to improve drying rate, or as a consequence of hydrodynamic limitations or reduction in condenser capacity.

Further improvements have to be made in the monitoring and control algorithms, to take into account the effect of batch heterogeneity on the reliability of the sensors, especially those based on the pressure rise test, and on the performance of the control system. If an aggressive control policy, based on the estimation of the "mean" state of the batch, is used, a fraction of the product, that experiences higher temperatures, can be damaged; to avoid this, and to improve the uniformity inside each batch, and the inter-batch reproducibility, it is necessary to estimate, and to take into account, the variance of the lot: the development of software-sensors, that match a mathematical model with some physical measurements, and the use of wireless technology, can be a possible solution, compatible with the restrictions of industrial equipment that uses automatic loading and unloading systems.

Acknowledgements

The authors would like to acknowledge their coworkers Salvatore Velardi, Roberto Pisano, Valeria Rasetto, Daniele Marchisio, Alberto Vallan (Politecnico di Torino, Italy) who contributed greatly to most of the recent results presented. The contribution by Julien Andrieu (LAGEP-CPE, Lyon, France) and Miquel Galan (Telstar-Industrial, Spain) is also gratefully acknowledged. The European Union has partially supported our research activity in this field, in the framework of the research project LYO-PRO — Optimization and control of the freeze-drying of pharmaceutical proteins (GROWTH Project GRD1-2001-40259-RTD): this publication contributes to the dissemination of the "Suggestions for modification of equipment and control system for enhanced freeze-drying". Financial support by Telstar-Industrial (Spain) is also gratefully acknowledged.

Additional Notation Used in Chapter 4

C	stop coefficient (variation rate of the solvent in the product)	s^{-1}
F_{leak}	leakage rate	$Pa\,s^{-1}$
$\mathbf{f}, \mathbf{h}$	application from $\mathbb{R}^n \times \mathbb{R}^m$ to $\mathbb{R}^n$	
h_p	prediction horizon	s
Δh_s	enthalpy of sublimation	$J\,kg^{-1}$
i_{18}	ionic current corresponding to fragment of mass 18 measured by the QMS	A
K	permeability (effective diffusivity)	$m^2\,s^{-1}$
$\mathbf{K}$	gain of the observer	
K_I	tuning parameter for an integral controller	s^{-1}
K_P	tuning parameter for a proportional controller	
K_v	overall heat transfer coefficient	$J\,m^{-2}\,s^{-1}\,K^{-1}$
k_d	kinetic constant of the desorption reaction	s^{-1}
R	mass transfer resistance	$m\,s^{-1}$
r	heating/cooling rate	$K\,s^{-1}$
r_d	desorption rate	s^{-1}
T_g'	glass transition temperature	°C or K
t_N	time horizon	s
t_{N^*}	time at which the frozen layer thickness is equal to zero	s
$\mathbf{u}$	manipulated input of a system	
w	mass of water	kg
$\mathbf{x}$	state of a system	
$\mathbf{y}$	measured output of a system	

Greek Symbols

γ	correction coefficient accounting for batch heterogeneity in DPE algorithm
ε	error

Subscripts

B	sample bottom, corresponding to $z = L_{frozen}$
c	chamber
f	final value
i	interface ($z = 0$)
in	inert gas
p	product
s	stopper
sp	set-point
tot	total

v vial
0 value at $t = 0$

Superscripts

$\wedge$ estimation
(-1) PRT before the actual one
* allowed value

Abbreviations

BTM barometric temperature measurement
CFD computational fluid dynamics
DPE dynamic parameters estimation
DPM drying process monitoring
ISE integral of the square errors
NIR near-infrared
MPC model predictive control
MTM manometric temperature measurement
PAT process analytical technology
PI proportional integral
PRA pressure rise analysis
PRT pressure rise test
QMS quadrupole mass spectrometer
RTD resistance thermal detector

References

Armstrong, J. G., 1980. Use of the capacitance manometer gauge in vacuum freeze-drying. *J. Parent. Drug Assoc.* **34**: 473–483.

Bardat, A., Biguet, J., Chatenet, E., Courteille, F., 1993. Moisture measurement: a new method for monitoring freeze-drying cycles. *PDA J. Parent. Sci. Technol.* **47**: 293–299.

Barresi, A. A., Baldi, G., Parvis, M., Vallan, A., Velardi, S., Hammouri, H., 2007. Optimization and control of the freeze-drying process of pharmaceutical products. International Publication No. WO2007/116371 A2, World Intellectual Property Organization.

Barresi, A. A., Pisano, R., Rasetto, V., Fissore, D., Marchisio, D. L., Galan, M., 2008a. Model-based monitoring and controlling of industrial freeze-drying processes. *Proceedings of 16th International Drying Symposium-IDS2008* (ed. B.N. Thorat), Ramoji Film City, India, Volume B, 746–754.

Barresi, A. A., Rasetto, V., Pisano, R., Fissore, D., Marchisio, D. L., Vanni, M., 2008b. Multiscale modelling of freeze-drying for optimisation and quality control of pharmaceutical products. *Proceedings of 5th Chemical Engineering Conference for Collaborative Research in Eastern Mediterranean Countries - EMCC5*

(eds G. Iorio, V. Calabrò, S. Curcio, D. Gabriele, M. Migliorin). Cetraro, Italy, 390–393.

Barresi, A. A., Pisano, R., Fissore, D., Rasetto, V., Velardi, S. A., Vallan, A., Parvis, M., Galan, M., 2009a. Monitoring of the primary drying of a lyophilization process in vials. *Chem. Eng. Process.* **48**: 408–423.

Barresi, A. A., Velardi, S., Fissore, D., Pisano, R., 2009b. Monitoring and controlling processes with complex dynamics using soft sensors, in *Modeling, control, simulation and diagnosis of complex industrial and energy systems* (eds. L. Ferrarini, C., Veber). Chapter 7, pp. 139–162. O3NEDIA - ISA Series on Industrial Automation, Ottawa, Canada.

Barresi, A. A., Velardi, S. A., Pisano, R., Rasetto, V., Vallan, A., Galan, M., 2009c. In-line control of the lyophilization process. A gentle PAT approach using software sensors. *Int. J. Refrig.* **32**: 1003–1014.

Barresi, A. A., Pisano, R., Rasetto, V., Fissore, D., Marchisio, D. L., 2010. Model-based monitoring and control of industrial freeze-drying processes: effect of batch non-uniformity. *Drying Technol.* **28**: 577–590.

Becerra, V. M., Roberts, P. D., Griffiths, G. W., 2001. Applying the extended Kalman filter to systems described by non-linear differential-algebraic equations. *Control Eng. Pract.* **9**: 267–281.

Boss, E. A., Filho, R. M., Vasco de Toledo, E. C., 2004. Freeze drying process: real time model and optimization. *Chem. Eng. Process.* **43**: 1475–1485.

Bouldoires, J. P., 1969. Etude expérimentale des transferts de chaleur et de masse en cours de lyophilisation par mesures diélectriques et par mesure de pression de vapeur. *Proceedings of Symposium on Thermodynamic Aspects of Freeze-drying*, International Institute of Refrigeration, Cleveland, USA.

Brülls, M., Rasmuson, A., 2002. Heat transfer in vial lyophilization. *Int. J. Pharm.* **246**: 1–16.

Brülls, M., Folestad, S., Sparén, A., Rasmuson, A., 2003. In-situ near-infrared spectroscopy monitoring of the lyophilization process. *Pharmaceut. Res.* **20**: 494–499.

Bruttini, R., Rovero, G., Baldi, G., 1986. Impiego di un impianto pilota per lo studio cinetico di un processo di liofilizzazione. *Il farmaco. Edizione Pratica.* **11**: 346–357.

Bruttini, R., Rovero, G., Baldi, G., 1991. Experimentation and modelling of pharmaceutical lyophilisation using a pilot plant. *Chem. Eng. J.* **45**: 67–77.

Cavatur, R. K., Suryanarayanan, R, 1998. Characterization of phase transitions during freeze-drying by in situ X-ray powder diffractometry. *Pharm. Dev. Technol.* **3**: 579–586.

Chase, D. R., 1998. Monitoring and control of a lyophilization process using a mass flow controller. *Pharm. Eng.* **18**: 11–17.

Chouvenc, P., Vessot, S., Andrieu, J., Vacus, P., 2004. Optimization of the freeze-drying cycle: a new model for pressure rise analysis. *Drying Technol.* **22**: 1577–1601.

Chouvenc, P., Vessot, S., Andrieu, J., Vacus, P., 2005. Optimization of the freeze-drying cycle: adaptation of the Pressure Rise Analysis to non-instantaneous isolation valves. *PDA J. Pharm. Sci. Technol.* **5**: 298–309.

Christ, M., 1995. Freeze-drying plant. International Publication No. WO/1995/010744 A1, World Intellectual Property Organization.

Ciruczak, E. W., 2002. Growth of near-infrared spectroscopy in pharmaceutical and medical sciences. *Am. Pharm. Rev.* **5**: 68–73.

Connelly, J. P., Welch, J. V., 1993. Monitor lyophilization with mass spectrometer gas analysis. *J. Parent. Sci. Technol.* **47**: 70–75.

Corbellini, S., Parvis, M., Vallan, A., 2010. In-process temperature mapping system for industrial freeze-dryers. *IEEE Trans. Meas. Instr.* **59**: 1134–1140.

Couriel, B., 1977. Advances in lyophilization technology. *Bull. Parent. Drug Assoc.* **31**: 227–235.

Daraoui, N., Dufour, P., Hammouri, H., Hottot, A., 2008. Optimal operation of sublimation time of the freeze drying process by predictive control: application of the MPC@CB software. *Proceedings of 18th European Symposium on Computer Aided Process Engineering – ESCAPE18* (eds B. Braunschweig, X. Joulia). Lyon, France. *Computer-Aided Chemical Engineering* 25: 453–458, Elsevier, Amsterdam, Netherlands.

De Beer, T. R. M., Alleso, M., Goethals, F., Coppens, A., Heyden, Y. V., Lopez De Diego, H., Rantanen, J., Verpoort, F., Vervaet, C., Remon, J. P., Baeyens, W. R. G., 2007. Implementation of a process analytical technology system in a freeze-drying process using Raman spectroscopy for in-line process monitoring. *Anal. Chem.* **79**: 7992–8003.

De Luca, P., Lachman, L., 1965. Lyophilization of pharmaceuticals, I: Effect of certain physical–chemical properties. *J. Pharm. Sci.* **54**: 617–623.

Fissore, D., Velardi, S. A., Barresi, A. A., 2008a. In-line control of a freeze-drying process in vial. *Drying Technol.* **26**: 685–694.

Fissore, D., Barresi, A. A., Pisano, R., 2008b. Method for monitoring the secondary drying in a freeze-drying process. European Patent Application No. EP 2148158 A1.

Fissore, D., Pisano, R., Barresi, A. A., 2009a. On the design of an in-line control system for a vial freeze-drying process: the role of chamber pressure. *Chem. Prod. Proc. Model.* **4** (2): 1–20.

Fissore, D., Pisano, R., Rasetto, V., Marchisio, D. L., Barresi, A. A., Vallan, A., Corbellini, S., 2009b. Applying Process Analytical Technology (PAT) to the lyophilization process. *Chim. Oggi/Chem. Today.* **27** (2): VII–XI.

Fissore, D., Pisano, R., Velardi, S. A., Barresi, A. A., Galan, M., 2009c. PAT tools for the optimization of the freeze-drying process. *Pharm. Eng.* **29** (5): 58–70.

Fissore, D., Pisano, R., Barresi, A. A., 2011a. On the methods based on the Pressure Rise Test for monitoring a freeze-drying process. *Drying Technol.* **29**: 73–90.

Fissore, D., Pisano, R., Barresi, A. A., 2011b. Monitoring of the secondary drying in freeze-drying of pharmaceuticals. *J. Pharm. Sci.* **100**: 732–742.

Franks, F., 1998. Freeze-drying of bioproducts: putting principles into practice. *Eur. J. Pharm. Biopharm.* **45**: 221–229.

Franks, F., 2007. *Freeze-drying of pharmaceuticals and biopharmaceuticals.* Royal Society of Chemistry, Cambridge, UK.

Gan, K. H., Bruttini, R., Crosser, O. K., Liapis, A. A., 2004. Heating policies during the primary and secondary drying stages of the lyophilization process in vials: effects of the arrangement of vials in clusters of square and hexagonal arrays on trays. *Drying Technol.* **22**: 1539–1575.

Gan, K. H., Bruttini, R., Crosser, O. K., Liapis, A. A., 2005a. Freeze-drying of pharmaceuticals in vials on trays: effects of drying chamber wall temperature and tray side on lyophilization performance. *Int. J. Heat Mass Transfer* **48**: 1675–1687.

Gan, K. H., Crosser, O. K., Liapis, A. I., Bruttini, R., 2005b. Lyophilisation in vials on trays: effects of tray side. *Drying Technol.* **23**: 341–363.

Genin, N., Rene, F., Corrieu, G., 1996. A method for on-line determination of residual water content and sublimation end-point during freeze-drying. *Chem. Eng. Process.* **35**: 255–263.

Gieseler, H., 2004. *Product morphology and drying behavior delineated by a new freeze-drying microbalance.* Diss., University of Erlangen, Germany.

Gieseler, H., Lee, G., 2008a. Effects of vial packing density on drying rate during freeze-drying of carbohydrates or a model protein measured using a vial-weighing technique. *Pharm. Res.* **25**: 302–312.

Gieseler, H., Lee, G., 2008b. Effect of freeze-dryer design on drying rate of an amorphous protein-formulation determined with a vial-weighing technique. *Pharm. Dev. Technol.* **13**: 463–472.

Gieseler, H., Kessler, W. J., Finson, M., Davis, S. J., Mulhall, P. A., Bons, V., Debo, D. J., Pikal, M. J., 2007a. Evaluation of Tunable Diode Laser Absorption Spectroscopy for in-process water vapor mass flux measurement during freeze drying. *J. Pharm. Sci.* **96**: 1776–1793.

Gieseler, H., Kramer, T., Pikal, M. J., 2007b. Use of Manometric Temperature Measurement (MTM) and SMART™ Freeze Dryer technology for development of an optimized freeze-drying cycle. *J. Pharm. Sci.* **96**: 3402–3418.

Hammerer, K., 2007. Wireless temperature-measurement as an innovative PAT-method. *Proceedings of 2nd Congress on Life*

Science Process Technology, Nuremberg, Germany.

Hottot, A., Vessot, S., Andrieu, J., 2005. Determination of mass and heat transfer parameters during freeze-drying cycles of pharmaceutical products. *PDA J. Pharm. Sci. Technol.* **59**: 138-1-53.

Hottot, A., Peczalski, R., Vessot, S., Andrieu, J., 2006. Freeze-drying of pharmaceutical proteins in vials: modeling of freezing and sublimation steps. *Drying Technol.* **24**: 561–570.

Hottot, A., Vessot, S., Andrieu, J., 2007. Freeze drying of pharmaceuticals in vials: influence of freezing protocol and sample configuration on ice morphology and freeze-dried cake texture. *Chem. Eng. Process.* **46**: 666–674.

Hottot, A., Andrieu, J., Hoang, V., Shalaev, E. Y., Gatlin, L. A., Rickett, F. S., 2009. Experimental study and modelling of freeze-drying in syringe configuration, Part II: Mass and heat transfer parameters and sublimation end-points. *Drying Technol.* **27**: 49–58.

Hsu, C. C., Ward, Carole F A., Pearlman, R., Nguyen, H. M., Yeung, D. A., Curley, J. G., 1992. Determining the optimum residual moisture in lyophilized protein pharmaceuticals. *Dev. Biol. Standard* **74**: 255–271.

Jefferis R. P., III, 1981. Control of biochemical recovery processes. *Ann. NY Acad. Sci.* **369**: 275–284.

Jefferis R. P., III, 1983. The microcomputer control of lyophilization. *Ann. NY Acad. Sci.* **413**: 283–289.

Jennings, T. A., 1980. Residual gas analysis and vacuum freeze drying. *J. Parent. Drug Assoc.* **34**(3): 62–69.

Jennings, T. A., 1982. Method and apparatus for determining the low temperature characteristics of materials. United States Patent No. 4327573.

Jennings, T. A., 1986. Effect of pressure on the sublimation rate of ice. *J. Parent. Sci. Technol.* **4**: 95–97.

Jennings, T. A., 1999. *Lyophilization: Introduction and basic principles*. Interpharm/CRC Press, Boca Raton, USA.

Jennings, T. A., Duan, N., 1995. Calorimetric monitoring of lyophilization. *PDA J. Pharm. Sci. Technol.* **49**: 272–282.

Kan, B., 1962. Methods of determining freeze-drying process end-points, in *Freeze-drying of foods* (ed. F. R. Fisher). National Academy of Sciences - National Research Council, Washington, D. C., USA, pp. 163–177.

Kessler, W. J., Davis, S. J., Mulhall, P. A., Silva, M., Pikal, M. J., Luthra, S., 2004. Lyophilizer monitoring using Tunable Laser Absorption Spectroscopy. *Proceedings of 18th International Forum Process Analytical Chemistry*, Arlington (VA), USA.

Kessler, W. J., Caledonia, G., Finson, M., Cronin, J., Paulsen, D., Davis, S. J., Mulhall, P. A., Gieseler, H., Schneid, S., Pikal, M. J., Schaepman, A., 2008. TDLAS-based mass flux measurements: critical analysis issues and product temperature measurements. *Proceedings of Freeze-drying of Pharmaceuticals and Biologicals Conference*, Breckenridge (CO), USA.

Kobayashi, M., Harashima, K., Sunama, R., Yao, A. R. (1991). Inter-vial variance of the sublimation rate in shelf freeze-dryer. *Proceedings of 18th International Refrigeration Congress*, Saint Hyacinthe (Quebec), Canada, 1711–1715.

Kuu, W. Y., Nail, S. L., Sacha, G., 2009. Rapid determination of vial heat transfer parameters using tunable diode laser absorption spectroscopy (TDLAS) in response to step-changes in pressure set-point during freeze-drying. *J. Pharm. Sci.* **98**: 1136–1154.

Lambert, W. J., Wang, Z., 2003. System and method for measuring freeze dried cake resistance. United States Patent No. 6643950 B2.

Leebron, K. S., Jennings, T. A., 1981. Determination of the vacuum outgassing properties of elastic closures by mass spectrometry. *J. Parent. Sci. Technol.* **35**: 100–105.

Liapis, A. I., 1987. Freeze drying, in *Handbook of industrial drying* (ed. A. S. Mujumdar,). Marcel Dekker Inc., New York, USA.

Liapis, A. I., Bruttini, R., 1995. Freeze-drying of pharmaceutical crystalline and amorphous solutes in vials: dynamic multi-dimensional models of the primary and secondary drying stages and qualitative features of the moving interface. *Drying Technol.* **13**: 43–72.

Liapis, A. I., Litchfield, R. J., 1979. Optimal control of a freeze dryer, I: Theoretical development and quasi steady-state analysis. *Chem. Eng. Sci.* **34**: 975–981.

Liapis, A. I., Sadikoglu, H., 1998. Dynamic pressure rise in the drying chamber as a remote sensing method for monitoring the temperature of the product during the primary drying stage of freeze-drying. *Drying Technol.* **16**: 1153–1171.

Liapis, A. I., Pikal, M. J., Bruttini, R., 1996. Research and development needs and opportunities in freeze-drying. *Drying Technol.* **14**: 1265–1300.

Litchfield, R. J., Liapis, A. I., 1982. Optimal control of a freeze dryer, II: Dynamic analysis. *Chem. Eng. Sci.* **37**: 45–55.

Livesey, R. G., Rowe, T. W. G., 1987. A discussion of the effect of chamber pressure on heat and mass transfer in freeze-drying. *J. Parent. Sci. Technol.* **41**: 169–171.

Lombraña, J. I., Diaz, J. M., 1987a. Heat programming to improve efficiency in a batch freeze-dryer. *Chem. Eng. J.* **35**: B23–B30.

Lombraña, J. I., Diaz, J. M., 1987b. Coupled vacuum and heating power control for freeze-drying time reduction of solutions in phials. *Vacuum*, **37**: 473–476.

Lombraña, J. I., De Elvira, C., Villaran, M. C., Izcara, J., 1993a. Simulation and design of heating profiles in heat controlled freeze-drying of pharmaceuticals in vials by the application of a sublimation semispherical model. *Drying Technol.* **11**: 471–487.

Lombraña, J. I., De Elvira, C., Villaran, M. C., 1993b. Simulation and design of heating profiles in heat controlled freeze-drying of pharmaceuticals in vials by the application of a sublimation cylindrical model. *Drying Technol.* **11**: 85–102.

Mackenzie, A. P., 1964. Apparatus for microscopic observations during freeze-drying. *Biodynamica* **9**: 213–222.

Mayeresse, Y., Veillon, R., Sibille, P. H., Nomine, C., 2007. Freeze-drying process monitoring using a cold plasma ionization device. *PDA J. Pharm. Sci. Technol.* **61**: 160–174.

Mellor, J. D., 1978. *Fundamentals of freeze-drying*. Academic Press, London, UK.

Milton, N., Pikal, M. J., Roy, M. L., Nail, S. L., 1997. Evaluation of manometric temperature measurement as a method of monitoring product temperature during lyophilisation. *PDA J. Pharm. Sci. Technol.* **5**: 7–16.

Monteiro Marques, J. P., Le Loch, C., Wolff, E., Rutledge, D. N., 1991. Monitoring freeze-drying by low resolution NMR: Determination of sublimation endpoint. *J. Food Sci.* **56**: 1707–1728.

Morris, J., Morris, G. J., Taylor, R., Zhai, S., Slater, N. K. H., 2004. The effect of controlled nucleation on ice structure, drying rate and protein recovery in vials in a modified freeze dryer. *Cryobiology* **49**: 308–309.

Nail, S. L., 1980. The effect of chamber pressure on heat transfer in the freeze-drying of parenteral solutions. *J. Parent. Drug Assoc.* **34**: 358–368.

Nail, S. L., Gatlin, L. A., 1985. Advances in control of production freeze-dryers. *J. Parent. Sci. Technol.* **39**: 16–27.

Nail, S. L., Gatlin, L. A., 1993. Freeze drying: Principles and practice, in *Pharmaceutical dosage forms*, Vol. **2** (eds A. Avis, A. Liebermann, L. Lachmann). Marcel Dekker Inc., New York, USA.

Nail, S. L., Johnson, W., 1991. Methodology for in-process determination of residual water in freeze-dried products. *Dev. Biol. Standard.* **74**: 137–151.

Nakagawa, K., Vessot, S., Hottot, A., Andrieu, J., 2006. Influence of controlled nucleation by ultrasounds on ice morphology of frozen formulations for pharmaceutical proteins freeze-drying. *Chem. Eng. Process.* **45**: 783–791.

Neumann, K. H., 1961. Freeze-drying apparatus. United States Patent No. 2994132.

Neumann, K. H., 1963. Temperature responsive freeze drying method and apparatus. United States Patent No. 3077036.

Neumann, K. H., 1968. Determining temperature of ice, in *Freeze-drying of Foods and Biologicals* (ed. R. Noyes). Noyes Development Corp., Park Ridge, USA.

Obert, J. P., 2001. *Modélisation, optimisation et suivi en ligne du procédé*

de lyophilisation: Application à l'amélioration de la productivité et de la qualité de bactéries lactiques lyophilisées. Diss., INRA, Paris-Grignon, France.

Oetjen, G. W., 1999. *Freeze-Drying*, Wiley-VCH, Weinheim, Germany.

Oetjen, G. W., 2001. Method of determining residual moisture content during secondary drying in a freeze-drying process. United States Patent No. 6176121 B1.

Oetjen, G. W., Schilder, G, 2003. In process moisture control within narrow end limits during freeze-drying of proteins. *PDA Annual Meeting*, Atlanta, USA.

Oetjen, G. W., Haseley, P., 2004. *Freeze-Drying*, 2nd edn, Wiley-VCH, Weinheim, Germany.

Oetjen, G. W., Ehlers, H., Hackenberg, U., Moll, J., Neumann, K. H., 1962. Temperature-measurement and control of freeze-drying processes, in *Freeze-drying of foods* (ed. F. R. Fisher). National Academy of Sciences - National Research Council, Washington, D. C., USA, pp. 178–190.

Oetjen, G. W., Haseley, P., Klutsch, H., Leineweber, M., 2000. Method for controlling a freeze-drying process. United States Patent No. 6163979 A1.

Passot, S., Fonseca, F., Trelea, I. C., Remillieux, A., Galan, M., Morris, G. J., Marin, M., 2007. Controlled nucleation improves efficiency of pharmaceutical protein lyophilization. *Proceedings of the Joint Conference of AFSIA and Drying Working Group of EFCE*, Biarritz, France, 54–55.

Patapoff, T. W., Overcashier, D. E., 2002. The importance of freezing on lyophilization cycle development. *BioPharm*. **3**: 16–21.

Pikal, M. J., Shah, S., 1990. The collapse temperature in freeze drying: dependence on measurement methodology and rate of water removal from the glassy phase. *Int. J. Pharm*. **62**: 165–186.

Pikal, M. J., Roy, M. L., Shah, S., 1984. Mass and heat transfer in vial freeze-drying of pharmaceuticals: role of the vial. *J. Pharm. Sci*. **73**: 1224–1237.

Pikal, M. J., Tang, X., Nail, S. L., 2005. Automated process control using manometric temperature measurement. United States Patent No. 6971187 B1.

Pisano, R., Fissore, D., Barresi, A. A., 2010b. On the use of a MPC algorithm for the in-line optimization of a pharmaceutical freeze-drying process. *Drying 2010 – Proceedings of the 17th International Drying Symposium (IDS 2010)* (eds E. Tsotsas, T. Metzger, M. Peglow), Magdeburg, Germany. Vol. A, 628–634.

Pisano, R., 2009. *Monitoring and control of a freeze-drying process of pharmaceutical products in vials*. Diss., Politecnico di Torino, Italy.

Pisano, R., Rasetto, V., Petitti, M., Barresi, A. A., Vallan, A., 2008. Modelling and experimental investigation of radiation effects in a freeze-drying process. *Proceedings of 5th Chemical Engineering Conference for Collaborative Research in Eastern Mediterranean Countries – EMCC5* (eds F. Scura, M. Liberti, G. Barbieri, E. Drioli). Cetraro, Italy, 394–397.

Pisano, R., Guler, S. B., Barresi, A. A., 2009. In-line detection of endpoint of sublimation in a freeze-drying process. *Proceedings of the Joint Conference of AFSIA and Drying Working Group of EFCE*, Lyon, France, ***Cahier de l'AFSIA* Nr. 23**: 110–111.

Pisano, R., Fissore, D., Velardi, S., Barresi, A. A., 2010a. In-line optimization and control of an industrial freeze-drying process for pharmaceuticals. *J. Pharm. Sci*. **99**: 4691–4709.

Ploechinger, H, Salzberger, F. P., 2006. Advanced Pirani gauges: engineers take Pirani gauges to a new level of performance. *R&D Magazine*, March 2006.

Presser, I., 2003. *Innovative online measurement procedures to optimize freeze-drying processes*. Diss., University of Munich, Germany.

Presser, I., Denkinger, N., Hoermann, H., Winter, G., 2002a. New methods in monitoring of freeze drying: near infrared spectroscopy determination of residue moisture during freeze drying. *Proceedings of Protein Stability Conference*, Breckenridge (CO), USA.

Presser, I., Denkinger, N., Hoermann, H., Winter, G., 2002b. New methods in monitoring of freeze drying: the use of mass spectrometer gas analysis to develop freeze-drying processes. *Proceedings of 4th World Meeting on Pharmaceutics, Biopharmaceutics*

and Pharmaceutical Technology, Florence, Italy.

Rambhatla, S., Ramot, R., Bhugra, C., Pikal, M. J., 2004. Heat and mass transfer scale-up issues during freeze drying, II: Control and characterization of the degree of supercooling. *AAPS Pharm. Sci. Technol.* **5**: article 58, 9 pp.

Rambhatla, S., Obert, J. P., Luthra, S., Bhugra, C., Pikal, M. J., 2005. Cake shrinkage during freeze drying: a combined experimental and theoretical study. *Pharm. Dev. Technol.* **1**: 33–40.

Rasetto, V., 2009. *Use of mathematical models in the freeze-drying field: process understanding and optimal equipment design.* Diss., Politecnico di Torino, Italy.

Rasetto, V., Marchisio, D. L., Fissore, D., Barresi, A. A., 2008. Model-based monitoring of a non-uniform batch in a freeze-drying process. *Proceedings of 18th European Symposium on Computer Aided Process Engineering – ESCAPE18* (eds B. Braunschweig, X. Joulia). Lyon, France. *Computer-Aided Chemical Engineering* 25: Paper FP_00210, CD Edition. Elsevier, Amsterdam, Netherlands.

Rasetto, V., Marchisio, D. L., Barresi, A. A., 2009. Analysis of the fluid-dynamics of the drying chamber to evaluate the effect of pressure and composition gradients on the sensor response used for monitoring the freeze-drying process. Proceedings of *European Drying Conference AFSIA 2009*, Lyon, France, ***Cahier de l'AFSIA*** **Nr. 23**, 89–99.

Rasetto, V., Marchisio, D. L., Fissore, D., Barresi, A. A., 2010. On the use of a dual-scale model to improve understanding of a pharmaceutical freeze-drying process. *J. Pharm. Sci.* **99**: 4337–4350.

Remmele, R. L., Stushnoff, C., Carpenter, J. F., 1997. Real-time in situ monitoring of lysozyme during lyophilization using infrared spectroscopy: Dehydration stress in the presence of sucrose. *Pharmaceut. Res.* **14**: 1548–1555.

Rene, F., Wolff, E., Rodolphe, F., 1993. Vacuum freeze-drying of a liquid in a vial: determination of heat and mass-transfer coefficients and optimisation of operating pressure. *Chem. Eng. Process.* **32**: 245–251.

Rene, F., Genin, N., Corrieu, G., 1995. Procédé et dispositif de contrôle de la lyophilisation sous vide. International Publication No. WO/1995/30118, World Intellectual Property Organization.

Rey, L. R., 1961. Automatic regulation of the freeze-drying of complex systems. *Biodynamica* **8**: 241–260.

Rey, L. P., 1963. Preserving water-containing organic or inorganic substances. United States Patent No. 3078586.

Rey, L. R., 1976. Glimpses into the fundamental aspects of freeze-drying. *Dev. Biol. Standard* **36**: 19–27.

Rey, L., May, J. C., 2004. *Freeze-drying/ lyophilization of pharmaceutical and biological products.* Marcel Dekker Inc., New York, USA.

Rieutord, L. M. A., 1965. Apparatus for regulating freeze-drying operations. United States Patent No. 3192643.

Roth, C., Winter, G., Lee, G., 2001. Continuous measurement of drying rate of crystalline and amorphous systems during freeze-drying using an in situ microbalance technique. *J. Pharm. Sci.* **90**: 1345–1355.

Rovero, G., Ghio, S., Barresi, A. A., 2001. Development of a prototype capacitive balance for freeze-drying studies. *Chem. Eng. Sci.* **56**: 3575–3584.

Roy, M. L., Pikal, M. J., 1989. Process control in freeze drying: determination of the end point of sublimation drying by an electronic moisture sensor. *J. Parent. Sci. Technol.* **43**: 60–66.

Rowe, T. D., 1990. A technique for the nucleation of ice. *Proceedings of International Symposium on Biological Product Freeze-Drying and Formulation*, Geneva, Switzerland.

Sadikoglu, H., 2005. Optimal control of the secondary drying stage of freeze drying of solutions in vials using variational calculus. *Drying Technol.* **23**: 33–57.

Sadikoglu, H., Liapis, A. I., 1997. Mathematical modelling of the primary and secondary stages of bulk solution freeze-drying in trays: parameter estimation and model discrimination by comparison of theoretical results with experimental data. *Drying Technol.* **13**: 43–72.

Sadikoglu, H., Liapis, A. I., Crosser, O. K., 1998. Optimal control of the primary and

secondary drying stages of bulk solution freeze drying in trays. *Drying Technol.* **16**: 399–431.

Sadikoglu, H., Ozdemir, M., Seker, M., 2003. Optimal control of the primary drying stage of freeze drying of solutions in vials using variational calculus. *Drying Technol.* **21**: 1307–1331.

Sadikoglu, H., Ozdemir, M., Seker, M., 2006. Freeze-drying of pharmaceutical products: Research and development needs. *Drying Technol.* **24**: 849–861.

Sandall, O. C., Wilke, C. R., 1967. The relationship between transport properties and rates of freeze drying poultry meats. *AIChE J.* **12**: 428–438.

Schelenz, G., Engel, J., Rupprecht, H., 1994. Sublimation drying lyophilization detected by temperature profile and X-ray technique. *Int. J. Pharm.* **113**: 133–140.

Schneid, S., Gieseler, H., 2008. Evaluation of a new wireless temperature remote interrogation system (TEMPRIS) to measure product temperature during freeze drying. *AAPS Pharm. Sci. Technol.* **9**: 729–739.

Schneid, S., Gieseler, H., Kessler, W., Pikal, M. J., 2007. Tunable Diode Laser Absorption Spectroscopy (TDLAS) as a residual moisture monitor for the secondary drying stage of freeze-drying. *Proceedings of AAPS Annual Meeting and Exposition*, San Diego (CA), USA.

Schneid, S., Gieseler, H., Kessler, W. J., Pikal, M. J., 2009. Non-invasive product temperature determination during primary drying using Tunable Diode Laser Absorption Spectroscopy. *J. Pharm. Sci.* **98**: 3406–3418.

Searles, J. A., Carpenter, J. F., Randolph, T. W., 2001a. The ice nucleation temperature determines the primary drying rate of lyophilization for samples frozen on a temperature-controlled shelf. *J. Pharm. Sci.* **90**: 860–871.

Searles, J. A., Carpenter, J. F., Randolph, T. W., 2001b. Annealing to optimize the primary drying rate, reduce freezing-induced drying rate heterogeneity, and determine T_g' in pharmaceutical lyophilization. *J. Pharm. Sci.* **90**: 872–887.

Sennhenn, B., Gehrmann, D., Firus, A., 2005. Freeze drying apparatus. United States Patent No. 6931754 B2.

Skibsted, E., 2006. Near infrared spectroscopy: the workhorse in the PAT toolbox. *Spectroscopy Europe* **18**: 14–17.

Suherman, P. M., Taylor, P. M., Smith, G., 2002. Development of a remote electrode system for monitoring the water content of materials inside a glass vial. *Pharmaceut. Res.* **19**: 337–344.

Tang, X., Pikal, M. J., 2004. Design of freeze-drying processes for pharmaceuticals: practical advice. *Pharmaceut. Res.* **21**: 191–200.

Tang, X. C., Nail, S. L., Pikal, M. J., 2005. Freeze-drying process design by manometric temperature measurement: design of a smart freeze-dryer. *Pharmaceut. Res.* **22**: 685–700.

Tang, X. C., Nail, S. L., Pikal, M. J., 2006a. Evaluation of manometric temperature measurement, a Process Analytical Technology tool for freeze-drying, Part I: Product temperature measurement. *AAPS Pharm. Sci. Technol.* **7**: article 14, 9 pp.

Tang, X. C., Nail, S. L., Pikal, M. J., 2006b. Evaluation of manometric temperature measurement, a Process Analytical Technology tool for freeze-drying, Part II: Measurement of dry layer resistance. *AAPS Pharm. Sci. Technol.* **7**: article 93, 8 pp.

Tang, X. C., Nail, S. L., Pikal, M. J., 2006c. Evaluation of manometric temperature measurement (MTM), a Process Analytical Technology tool in freeze drying, Part III: Heat and mass transfer measurement. *AAPS Pharm. Sci. Technol.* **7**: article 97, 7 pp.

Tenedini, K. J., Bart S. G., Jr., 2001. Freeze drying methods employing vapor flow monitoring and/or vacuum pressure control. United States Patent No. 6226997 B1.

Thompson, T. N., 1988. Process and device for determining the end of primary stage of freeze drying. United States Patent No. 4780964.

Trelea, I. C., Passot, S., Fonseca, F., Marin, M., 2007. An interactive tool for the optimization of freeze-drying

cycles based on quality criteria. *Drying Technol.* **25**: 741–751.

Vallan, A., 2007. A measurement system for lyophilization process monitoring. *Proceedings of Instrumentation and Measurement Technology Conference - IMTC 2007*, Warsaw, Poland, IEEE: Piscataway, USA. doi: 10.1109/IMTC.2007.379000

Vallan, A., Corbellini, S., Parvis, M., 2005a. A Plug&Play architecture for low-power measurement systems. *Proceedings of Instrumentation and Measurement Technology Conference - IMTC 2005*, Ottawa, Canada, Volume 1, 565–569.

Vallan, A., Parvis, M., Barresi, A. A., 2005b. Sistema per la misurazione in tempo reale di massa e temperatura di sostanze sottoposte a liofilizzazione. Italian Patent Application No. B02005A000320.

Velardi, S. A., Barresi, A. A., 2008a. Development of simplified models for the freeze-drying process and investigation of the optimal operating conditions. *Chem. Eng. Res. Des.* **86**: 9–22.

Velardi, S. A., Barresi, A. A., 2008b. Method and system for controlling a freeze drying process. International Publication No. WO/2008/034855, World Intellectual Property Organization.

Velardi, S. A., Barresi, A. A., Hottot, A., Andrieu, J., 2005. Pharmaceuticals freeze-drying in vials: a new heat transfer model including the effect of the vial sidewall. *Proceedings of the Joint Conference of AFSIA and Drying Working Group of EFCE*, Paris, France, 20–21.

Velardi, S. A., Rasetto, V., Barresi, A. A., 2008. Dynamic Parameters Estimation Method: advanced Manometric Temperature Measurement approach for freeze-drying monitoring of pharmaceutical. *Ind. Eng. Chem. Res.* **47**: 8445–8457.

Velardi, S. A., Hammouri, H., Barresi, A. A., 2009. In-line monitoring of the primary drying phase of the freeze-drying process in vial by means of a Kalman filter based observer. *Chem. Eng. Res. Des.* **27**: 1409–1419.

Velardi, S., Hammouri, H., Barresi, A. A., 2010. Development of a High Gain observer for in-line monitoring of sublimation in vial freeze-drying. *Drying Technol.* **28**: 256–268.

Wang, W., 2000. Lyophilization and development of solid protein pharmaceuticals. *Int. J. Pharm.* **203**: 1–60.

Wiggenhorn, M., Winter, G., Presser, I., 2005a. The current state of PAT in freeze-drying. *Am. Pharm. Rev.* **8**: 38–44.

Wiggenhorn, M., Presser, I., Winter, G., 2005b. The current state of PAT in freeze-drying. *Eur. Pharm. Rev.* **10**: 87–92.

Wiggenhorn, M., De Beer, T., Geier, F., Baeyens, W. R. G., Winter, G., Freiss, W., 2008. Evaluation of advanced approaches to monitor product temperature during lyophilization and the implementation of process analyzers (PAT). *Proceedings of Freeze-drying of Pharmaceuticals and Biologicals Conference*, Breckenridge (CO), USA.

Willemer, H., 1987. Additional independent process control by process sampling for sensitive biomedical products. *Proceedings of 17° Congrès International du Froid*, (I.I.R., Paris), Wien, Austria, Volume C, 146–152.

Willemer, H., 1991. Measurement of temperature, ice evaporation rates and residual moisture contents in freeze-drying. *Dev. Biol. Standard* **74**: 123–136.